

MAXIMUM POWER POINT TRACKING USING IMPROVED PERTURB AND  
OBSERVE TECHNIQUE STAND-ALONE PHOTOVOLTAIC SYSTEM

ASBAN DOLAH

UNIVERSITI TEKNOLOGI MALAYSIA

MAXIMUM POWER POINT TRACKING USING IMPROVED PERTURB AND  
OBSERVE TECHNIQUE STAND-ALONE PHOTOVOLTAIC SYSTEM

ASBAN DOLAH

A thesis submitted in fulfilment of the  
requirements for the award of the degree of  
Doctor of Philosophy

Razak Faculty of Technology and Informatics  
Universiti Teknologi Malaysia

SEPTEMBER 2021

## **DEDICATION**

This thesis is dedicated to my family, who taught me that the best kind of knowledge to have is that which is learned for its own sake. It is also dedicated to my wife, who taught me that even the largest task can be accomplished if it is done one step at a time.

## ACKNOWLEDGEMENT

In preparing this thesis, I spoke with a lot of people while writing this thesis, including researchers, academics, and practitioners. They have aided my comprehension and thoughts. I'd like to express my heartfelt gratitude to my main thesis supervisor, Professor Dr. Rasli bin Abd Ghani, for his encouragement, guidance, criticism, and friendship. I am also grateful to Professor Dr. Yussof bin Wahab, my previous supervisor, for his guidance, advice, and motivation. This thesis would not have been the same without their continued support and interest.

I am also grateful to Universiti Teknologi Malaysia (UTM) for supporting my Ph.D. research. Staff at UTM and Telekom Research and Development should also be thanked for their assistance in providing relevant literature.

My fellow postgraduate students should also be acknowledged for their assistance. My heartfelt gratitude also goes out to all of my colleagues and others who have helped me on various occasions. Their perspectives and advice are extremely beneficial. Unfortunately, in this limited space, it is not possible to list all of them. I am grateful to every member of my family.

## ABSTRACT

Solar photovoltaic systems for off-grid power applications are widely used in rural lighting, telecommunication base stations, and remote monitoring among others. The base stations or remote antenna units (RAU) of the fibre-wireless (FiWi) system are deployed in remote or blind-spot urban areas where grid connected power supplies are unavailable. Therefore, the use of a stand-alone photovoltaic system is required. The different power output of photovoltaic cells due to weather conditions in Malaysia can cause severe problems in power efficiency and performance of solar power system. The Perturbation and Observation (P&O) method is a power-detection tracking technology that enables the DC-DC converter to work at Maximum Power Point (MPP). The main objective of the research is to improve the Maximum Power Point Tracking (MPPT) algorithm by improving P&O with variable step size for the buck converter to reach MPPT faster and more efficiently. The objective of the hardware section is to design and fabricate a DC-DC converter with a variable step size for use in the MPPT algorithm. In monitoring the performance of the DC-DC converter, measuring the output voltage that is close to its reference value should provide excellent accuracy of the converter. The proposed MPPT algorithm and DC-DC converter have been validated through simulations and experiments. The simulation and modelling of the photovoltaic cell have been conducted using MATLAB/Simulink®. The proposed models have been employed to predict the behaviour of the photovoltaic cell under different physical and environmental parameters. Based on the simulation results, the proposed method effectively reduces oscillations and simultaneously maintains sufficient tracking capability. The results also indicate that it is able to regulate MPPT, reduces oscillations, maintains the output voltage of the DC-DC converter at a constant state and provides better accuracy performance under rapid solar irradiance changes. The speed detected for MPPT is approximately 0.12 seconds. On average, the accuracy of power of the proposed method is substantially 98 per cent.

## ABSTRAK

Sistem fotovolta suria untuk aplikasi kuasa luar grid digunakan secara meluas dalam percahayaan di kawasan pendalaman, stesen pangkalan telekomunikasi, dan dalam kalangan pemantauan jarak jauh. Stesen pangkalan atau unit antena jarak jauh (RAU) bagi sistem “*fibre-wireless*” (FiWi) ditempatkan di kawasan terpencil atau titik buta kawasan bandar di mana bekalan kuasa yang terhubung grid tidak tersedia. Oleh itu, penggunaan sistem fotovolta berdiri sendiri diperlukan. Keluaran kuasa yang berbeza oleh sel-sel fotovolta disebabkan oleh keadaan cuaca di Malaysia boleh menyebabkan masalah teruk dalam kecekapan kuasa dan prestasi sistem kuasa suria. Kaedah Usikan dan Perhati (P&O) adalah pengesanan kuasa teknologi penjejakan yang membolehkan penukar DC-DC untuk berfungsi pada Titik Kuasa Maksimum (MPP). Objektif utama penyelidikan ini adalah untuk menambah baik algoritma Penjejakan Titik Kuasa Maksimum (MPPT) dengan memperbaiki P&O bersama saiz langkah berubah-ubah agar penukar “*buck*” mencapai MPPT cepat dan lebih cekap. Objektif bahagian perkakasan pula adalah mereka bentuk dan membina penukar DC-DC dengan saiz langkah berubah-ubah untuk digunakan dalam algoritma MPPT. Dalam pemantauan prestasi penukar DC-DC, mengukur voltan keluaran yang ia hampir dengan nilai rujukannya seharusnya memberikan ketepatan penukar yang sangat baik. Cadangan algoritma MPPT dan penukar DC-DC disahkan melalui proses simulasi dan ujikaji. Simulasi dan pemodelan sel fotovolta dijalankan menggunakan perisian MATLAB/Simulink®. Model yang dicadangkan berfungsi untuk meramal tingkah laku sel fotovolta di bawah parameter fizikal dan persekitaran yang berbeza. Berdasarkan keputusan simulasi, kaedah yang dicadangkan berkesan mengurangkan ayunan sambil mengekalkan kemampuan kecekapan penjejakan. Keputusan ujikaji pula menunjukkan bahawa ianya dapat mengawal atur MPPT, mengurangkan ayunan, mengekalkan voltan keluaran penukar DC-DC supaya sentiasa dalam keadaan malar, dan memberikan prestasi kejituan yang lebih baik di bawah kesinaran suria yang cepat. Kelajuan yang dikesan untuk MPPT adalah lebih kurang 0.12 saat. Secara purata, kejituan kuasa untuk kaedah yang dicadangkan adalah 98 peratus.

## TABLE OF CONTENTS

	TITLE	PAGE
	<b>DECLARATION</b>	<b>iii</b>
	<b>DEDICATION</b>	<b>iv</b>
	<b>ACKNOWLEDGEMENT</b>	<b>v</b>
	<b>ABSTRACT</b>	<b>vi</b>
	<b>ABSTRAK</b>	<b>vii</b>
	<b>TABLE OF CONTENTS</b>	<b>viii</b>
	<b>LIST OF TABLES</b>	<b>xii</b>
	<b>LIST OF FIGURES</b>	<b>xiv</b>
	<b>LIST OF ABBREVIATIONS</b>	<b>xviii</b>
	<b>LIST OF SYMBOLS</b>	<b>xx</b>
	<b>LIST OF APPENDICES</b>	<b>xxii</b>
<b>CHAPTER 1</b>	<b>INTRODUCTION</b>	<b>1</b>
1.1	Research Background	1
1.2	Problem Statement	3
1.3	Research Objectives	5
1.4	Strategy of Research	5
1.5	Outline of Thesis	7
<b>CHAPTER 2</b>	<b>LITERATURE REVIEW</b>	<b>9</b>
2.1	Introduction	9
2.2	Basic Concept of Photovoltaic (PV) System	9
2.3	Solar Photovoltaic (PV) Panel	10
2.4	Photovoltaic (PV) Cell Module	10
2.4.1	Effects of Solar Irradiance Variation	12
2.4.2	Effect of Varying Cell Temperature	13
2.4.3	Effect of Varying Series Resistance ( $R_s$ )	13
2.4.4	Effect of Varying Shunt Resistance ( $R_{sh}$ )	14

2.4.5	Array	14
2.5	Photovoltaic (PV) Fill Factor	14
2.6	Photovoltaic (PV) Efficiency	15
2.7	Maximum Power Point (MPP)	16
2.8	Maximum Power Point (MPP) Tracking	17
2.9	DC-DC Buck Converter Device	20
2.10	DC-DC Converter Efficiency	22
2.11	Maximum Power Point Tracking (MPPT) Control Technique	24
2.12	Types of Maximum Power Point Tracking (MPPT)	25
2.12.1	Perturbation and Observation (P&O) Method	25
2.12.2	Conventional Perturbation and Observation (P&O) Method	27
2.12.3	Modified Perturbation and Observation (P&O) Method	28
2.12.4	Improved Perturbation and Observation (P&O) Method	29
2.12.5	Proportional-Integral-Perturbation and Observation (PI- P&O) method	31
2.12.6	Incremental Conductance (INC) Method	34
2.12.7	Modified Incremental Conductance (INC) Algorithm	36
2.12.8	Incremental Conductance (INC) Method with Proportional Integral (PI) Regulator	38
2.12.9	Hybrid MPPT Method	39
2.12.10	Constant Voltage (CV) Method	42
2.13	Tracking Issue of MPPT	45
2.14	Summary	48
<b>CHAPTER 3</b>	<b>RESEARCH METHODOLOGY</b>	<b>49</b>
3.1	Introduction	49
3.2	Stand-Alone Solar System and Grid Connection	49
3.3	Stand-Alone Solar System (SASS)	50
3.4	Power Requirement for Remote Antenna Unit (RAU)	51
3.5	Stand-Alone Solar System Design Calculation	52



3.5.1	Step 1: Total Energy Required Daily	52
3.5.2	Step 2: Radiation Assumption	53
3.5.3	Step 3: System Voltage Consideration	53
3.5.4	Step 4: Total battery Bank Capacity Required Daily	53
3.5.5	Step 5: PV Array Size Considerations	54
3.6	Solar Module	55
3.7	DC-DC Converter Design	57
3.7.1	Inductor Selection	57
3.7.2	Capacitor Selection	59
3.8	DC-DC Converter Component Selection	60
3.8.1	Metal-Oxide-Semiconductor Transistor (MOSFET) Selection	60
3.8.2	Metal-Oxide-Semiconductor Transistor (MOSFET) Driver	61
3.8.3	Arduino Microcontroller	62
3.8.4	Current Measurement	62
3.8.5	Voltage Measurement	63
3.9	Design Schematics	64
3.10	Lithium Iron Phosphate (LiFePO <sub>4</sub> ) Batteries	67
3.11	PV System Design Summary	68
3.12	Fixed Step Size in P&O Method	69
3.13	Propose Variable Step Size in P&O Method	70
3.14	Summary	76
<b>CHAPTER 4</b>	<b>RESULTS AND DISCUSSION</b>	<b>77</b>
4.1	Introduction	77
4.2	Simulation Study	77
4.3	Test S1: Photovoltaic Simulation Test	78
4.3.1	Comparison between Two Different Approaches	78
4.3.2	Photovoltaic in Changing the Irradiance	82
4.3.3	Changing of Temperature	84
4.3.4	Changing of Series Resistance $R_S$	86

4.3.5	Photovoltaic in Series and Parallel	87
4.3.6	Photovoltaic Performance Simulation and Experiment	90
4.4	DC-DC Buck Converter Simulation	98
4.4.1	Test S2: European Standard Sequence (EN50530) Irradiance Profile Test under Single Sequence	100
4.4.2	Test S3: European Standard Sequence (EN50530) Irradiance Profile Test under Dynamic Sequence	103
4.4.3	Test S4: DC-DC Buck Converter Test	105
4.5	DC-DC Converter Performance Experiment	109
4.5.1	Test E1: Fixed Duty Cycle D and Small Step Size	111
4.5.2	Test E2: Ramp Down the Duty Cycle D and Decrease Step Size	118
4.5.3	Test E3: Suddenly Change Irradiance and Variable Step Size	124
4.6	Summary	129
<b>CHAPTER 5</b>	<b>CONCLUSION AND RECOMMENDATIONS</b>	<b>131</b>
5.1	Research Outcomes	131
5.2	Contributions to Knowledge	131
5.3	Future Works	133
	<b>REFERENCES</b>	<b>135</b>
	<b>LIST OF PUBLICATIONS</b>	<b>173</b>

## LIST OF TABLES

TABLE NO.	TITLE	PAGE
Table 2.1	List of research on P&O algorithms	33
Table 2.2	Summarized literature review of MPPT type (Dileep, <i>et al.</i> , 2017)	44
Table 2.3	Summary of Literature Review on MPPT Method	46
Table 3.1	System requirements for compact SASS with smart power management	51
Table 3.2	Electrical Performance at 1000 W/m <sup>2</sup> (STC) for KD135GH-2PU	55
Table 3.3	Electrical Performance at 1000 W/m <sup>2</sup> (STC) for TIF60W	56
Table 3.4	Electrical Performance at 1000 W/m <sup>2</sup> (STC) for TIF20W	56
Table 3.5	Components required for a complete PV module	68
Table 4.1	Electrical Characteristics for Both Approaches for Kyocera KD135GH-2PU	80
Table 4.2	Electrical Characteristics for Kyocera KD135GH-2PU from Simulation at 200, 600 and 1000 W/m <sup>2</sup>	84
Table 4.3	Maximum Characteristics at 600 and 1000 W/m <sup>2</sup> for Kyocera KD135GH-2PU	87
Table 4.4	Electrical Characteristics at Different Connections at 1000 W/m <sup>2</sup> for Kyocera KD135GH-2PU	90
Table 4.5	Maximum power for TIF60W	95
Table 4.6	Maximum power for TIF20W	98
Table 4.7	Steady State Value (SSV) and Slope Value (SV) of Irradiance	103
Table 4.8	Power panel, Duty cycle, and Accuracy for Converter at 548, 620 and 665 W/m <sup>2</sup>	109
Table 4.9	Duty cycle D for different levels of irradiance	117
Table 4.10	Converter performance at different levels of irradiance	117
Table 4.11	Duty cycle D ramped down from 0.85 to 0.65	122
Table 4.12	Converter performance at different irradiance	124

Table 4.13	Duty cycle D at different irradiance	127
Table 4.14	Converter Performance at different irradiance	127

## LIST OF FIGURES

FIGURE NO.	TITLE	PAGE
Figure 1.1	Overall FiWi system based on RoF deployment	2
Figure 1.2	Research methodology	7
Figure 2.1	PV cell equivalent circuit for Diode Model	11
Figure 2.2	Graf cell output current as a function of voltage	15
Figure 2.3	Maximum Power Point (MPP) at two different irradiance	17
Figure 2.4	Power-Voltage (P-V) Curve	18
Figure 2.5	Power Interface	18
Figure 2.6	Principle of the P&O method and the INC method	19
Figure 2.7	MOSFET is ON and OFF (a) Metal–Oxide–Semiconductor Field-Effect Transistor (MOSFET) is ON (b) Metal–Oxide–Semiconductor Field-Effect Transistor (MOSFET) is OFF	20
Figure 2.8	Diagram of a MOSFET switching signal	21
Figure 2.9	Inductance Current	22
Figure 2.10	MPP Tracking Method	24
Figure 2.11	The P&O algorithm flowchart for MPP Tracking	26
Figure 2.12	Various P&O block diagram topologies. (a) Conventional P&O with a fixed perturbation step. (b) Conventional P&O with adaptive perturbation step. (c) Modified P&O with fixed perturbation step. (d) Modified P&O with adaptive perturbation step. (Nabil, <i>et al.</i> , 2017)	27
Figure 2.13	Flowchart of the Classic P&O method (Liu, Y. <i>et al.</i> , 2014)	28
Figure 2.14	Flowchart of the Modified P&O Method (Ghassami, A.A. <i>et al.</i> , 2013)	29
Figure 2.15	Flowchart of the Improved P&O Method (Liu, Y. <i>et al.</i> , 2014)	30
Figure 2.16	Flowchart of the PI-P&O Method (Chen, P. <i>et al.</i> , (2015)	32
Figure 2.17	Flowchart of the INC algorithm (Ghassami, A. A. <i>et al.</i> , 2013)	35

Figure 2.18	The flowchart of the Modified INC Algorithm (Yan, Z. <i>et al.</i> , 2008)	37
Figure 2.19	INC Method MPPT with PI regulator	38
Figure 2.20	Flowchart of the Hybrid MPPT method (Jiang, J. <i>et al.</i> , 2014)	41
Figure 2.21	CV method flowchart (Liu, Y. <i>et al.</i> , 2014)	42
Figure 3.1	Stand-Alone Solar System (SASS) Simplified Block Diagram	50
Figure 3.2	Block diagram of a Stand-Alone Solar System (SASS)	55
Figure 3.3	Arduino Solar MPPT	56
Figure 3.4	Converter Power Stage	58
Figure 3.5	Resistor connection for voltage measurement	63
Figure 3.6	Schematic diagram for DC-DC converter	65
Figure 3.7	Schematic for input and output for Arduino	65
Figure 3.8	DC-DC Converter (a) Actual picture (b) Picture of PCB Board	66
Figure 3.9	Picture of Data Logger	67
Figure 3.10	Component level integration (60W Panel, MPPT DC-DC converter, LiFePO <sub>4</sub> battery and Data Tracker, Load)	68
Figure 3.11	The flowchart of the fixed step size P&O method	69
Figure 3.12	The flowchart of the variable step size in P&O method	70
Figure 3.13	Graph of power panel and $dP/dV$ verses voltage panel	71
Figure 3.14	Slopes of power versus voltage under 1000 and 200 W/m <sup>2</sup> irradiation conditions	72
Figure 3.15	The product of power and slope at different $M$ scaling	73
Figure 3.16	The product of power and slope at different irradiance	74
Figure 4.1	(a) Current versus voltage; (b) Power versus voltage, characteristics with varying irradiance for Kyocera KD135GH-2PU	79
Figure 4.2	PV system simulate (a) series connection; (b) parallel connection	81
Figure 4.3	Details of the interconnected PV Model	81
Figure 4.4	(a) Current versus voltage form simulation and technical specification Kyocera KD135GH-2PU and (b) Power	

	versus voltage for simulation characteristics with varying irradiance for Kyocera KD135GH-2PU	83
Figure 4.5	(a) Current versus voltage form simulation and technical specification Kyocera KD135GH-2PU and (b) Power versus voltage characteristics with varying temperature at 1000 W/m <sup>2</sup> for Kyocera KD135GH-2PU	85
Figure 4.6	(a) Current versus voltage and; (b) Power versus voltage characteristics with varying resistance for Kyocera KD135GH-2PU	87
Figure 4.7	(a) Current versus voltage and; (b) Power versus voltage characteristics with two panels in series connection for Kyocera KD135GH-2PU	88
Figure 4.8	(a) Current versus voltage and (b) Power versus voltage characteristics with two panels in parallel connection for Kyocera KD135GH-2PU	89
Figure 4.9	Tools for experiment (a) PROVA 200 Solar Module Analyzer (b) TES 1333R Solar Power Meter (c) Solar Panel TIF 60W and TIF 20W	91
Figure 4.10	Measurement and simulation results for TIF60W solar panel (a) I-V curve (b) P-V curve	94
Figure 4.11	Measurement and simulation results for TIF20W Solar Panel (a) I-V curve (b) P-V curve	98
Figure 4.12	(a) Physical model of PV Converter in Simulink (b) MPPT model in Simulink	99
Figure 4.13	A typical testing sequence of the European standard (Andrejas, T. <i>et al.</i> , 2011)	100
Figure 4.14	Irradiance profile for performance testing using MATLAB/Simulink® (Chen, P. <i>et al.</i> , 2015)	101
Figure 4.15	Simulation results for buck converter in test S2 (a) Panel power (b) Energy (Joule)	102
Figure 4.16	Irradiance profile for a step-like rapid change and steady state testing	104
Figure 4.17	Simulation results for Buck Converter Test S3 (a) Panel power (b) Calculation of Energy (Joule)	105
Figure 4.18	Graph for (a) Power panel (b) Current panel (c) Output voltage (d) Duty cycle D (e) Step size	108
Figure 4.19	Experimental setup (a) PV panel and Pyrometer (HT304N) (b) DC-DC converter Power Distribution Board and HT Solar-02 Solar Power Meter (c) Data logger	110

Figure 4.20	(a) Panel power tracking performance (b) Relation between output voltage and time (c) Duty cycle D tracking performance (d) Step size at different solar irradiance of 380, 422 and 548 W/m <sup>2</sup>	113
Figure 4.21	(a) Panel power tracking performance (b) Relation between output voltage and time (c) Duty cycle D tracking performance (d) Step size at different solar irradiance of 620 and 665 W/m <sup>2</sup>	116
Figure 4.22	Graph relation between duty cycle D and PWM	118
Figure 4.23	(a) Output voltage performance (b) Output power slope at different solar irradiance of 710, 715 and 840 W/m <sup>2</sup>	119
Figure 4.24	Graph of duty cycle D performance at different solar irradiance of 710, 715 and 840 W/m <sup>2</sup>	120
Figure 4.25	Graph of (a) Output voltage (b) Output power (c) Step size versus time at different solar irradiance of 710, 715 and 840 W/m <sup>2</sup>	122
Figure 4.26	Graph PV characteristics at different solar irradiance 710, 715 and 840 W/m <sup>2</sup>	123
Figure 4.27	Power panel-tracking performance at different solar irradiance of 800 and 850 W/m <sup>2</sup>	125
Figure 4.28	Graph of output voltage and time at different solar irradiance of 800 and 850 W/m <sup>2</sup>	125
Figure 4.29	Graph of duty cycle D and time at different solar irradiance of 800 and 850 W/m <sup>2</sup>	126
Figure 4.30	Graph of step size tracking performance at different solar irradiance 800 and 850 W/m <sup>2</sup>	126
Figure 4.31	Oscillation of P&O algorithm	128



## LIST OF ABBREVIATIONS

AC	-	Alternating current
ANN	-	Artificial Neural Network
BCR	-	Battery Component Replacement
BTS	-	Base Terminal Station
CCM	-	Continuous Conduction Mode
CS	-	Central Station
CV	-	Constant-Voltage
D	-	Duty Cycle
DC-DC	-	Direct Current to Direct Current
DCM	-	Discontinuous Conduction Mode
DOD	-	Depth of Discharge
DSP	-	Digital Signal Processing
DT	-	Duty Time
EA	-	Evolutionary Algorithms
FF	-	Fill Factor
FiWi	-	Fiber Wireless
FLC	-	Fuzzy Logic Control
G	-	Gega
GA	-	Genetic Algorithm
GSO	-	Golden Section Optimization
GW	-	Giga Watts
IC	-	Integrated Circuit
$I_{MPP}$	-	Current at Maximun Power Point
INC	-	Incremental Conductance
I-V	-	Current-Voltage
LCD	-	Liquid Crystal Display
LED	-	Light-Emitting Diode
$LiFePO_4$	-	Lithium Iron Phosphate
LPF	-	Low-Pass Filter
MCU	-	Micro-controller Unit
MOSFET	-	Metal–Oxide–Semiconductor Field-Effect Transistor
MPC	-	Model Predictive Controller
MPP	-	Maximum Power Point

MPPT	-	Maximum Power Point Tracking
MW	-	Mega Watts
OV	-	Open Voltage
P&O	-	Perturbation and Observation
PCM	-	Protection Circuits Module
PCM	-	Power Control Management
PGS	-	Parameter Guides System
PI	-	Proportional-Integral
PID	-	Proportional-Integral-Derivative
PSC	-	Partial Shade Condition
PV	-	Photovoltaic
P-V	-	Power-Voltage
PWM	-	Pulse Width Modulation
RAU	-	Remote Antenna Unit
$R_{DS}$	-	Drain to Source Resistance
RoF	-	Radio-over-Fiber
$R_P$	-	Paralel Resistance
$R_S$	-	Series Resistance
SASS	-	Stand-Alone Solar System
SD	-	Standard Deviation
SSO	-	Steady State Operation
SSV	-	Steady State Value
STC	-	Standard Test Condition
SV	-	Slope Value
SW	-	Switch
T	-	Tera
TS	-	Takagi-Sugeno
UV	-	Ultra Violet
$V_{MPP}$	-	Voltage at Maximun Power Point

## LIST OF SYMBOLS

$E_g$	-	Bang-gap Energy
$I_D$	-	Current Shunted
$I_{PV}$	-	Photovoltaic Output Current
$I_{rs}$	-	Cell's Reverse Saturation Current
$I_{sc}$	-	Short-circuit Current
$N_p$	-	Number Parallel of Cells
$N_S$	-	Number Series of Cells
$R_S$	-	Series Resistance
$R_{SH}$	-	Shunt resistance
$T_c$	-	Junction Temperature
$T_{ref}$	-	Cell's Reference Temperature
$\Delta I$	-	Delta Ripple current
$\Delta V$	-	Delta Voltage
$A$	-	Ideal Factor
$Area$	-	Cell Area
$C$	-	Capacitor
$C_{1/2}$	-	Product Power and $dP/dV$
$C_{out}$	-	Output Capacitance
$D$	-	Duty Cycle
$DT$	-	Duration Time
$e$	-	error
$E$	-	Energy
$E_{DC}$	-	Total Energy Required Daily for DC Load
$E_{required\ daily}$	-	total energy required daily
$F_{ideal}$	-	Ideal Maximum Expected Power
$f_{sw}$	-	Switching Frequency
$G_a$	-	Ambient Irradiation
$iL$	-	Inductance Current
$I_{dss}$	-	Drain-to-Source Leakage Current
$I_{max}$	-	Current at Maximum
$I_{out}$	-	Output Current
$J_{mp}$	-	Current Flux
$K$	-	Boltzmann's Constants

$K_I$	-	Constant
$K_i$	-	Integral Gain
$K_p$	-	Proportional Gain
$L$	-	Inductor
$M$	-	Scaling Factor
$\eta$	-	Efficiency
$P_{con}$	-	Operating Power Consumption
$P_{in}$	-	Input Power
$P_{max}$	-	Maximum Power
$P_{out}$	-	Output Power
$P_{PV}$	-	Panel Power
$R_{DS}$	-	Drain to Source Resistance
$R_O$	-	Load Resistance at MPP
$R_P$	-	Resistance PV
$R_T$	-	Load Resistance any Intersect I-V Curve
$t$	-	Number of Hours is in Use (h)
$T$	-	Time
$T_{op}$	-	Operating Temperature
$V_{dc}$	-	Direct Current Voltage
$V_{dss}$	-	Drain-to-Source Breakdown Voltage
$V_i$	-	Input Voltage
$V_{max}$	-	Voltage at Maximum
$V_O$	-	Output Voltage
$V_{oc}$	-	Open-circuit Voltage
$V_{out}$	-	Output Voltage
$V_{pv}$	-	Panel Voltage
$V_{ref}$	-	Reference Voltage
$\beta$	-	Power Slope

## LIST OF APPENDICES

<b>APPENDIX</b>	<b>TITLE</b>	<b>PAGE</b>
Appendix A	Actual Equipment	143
Appendix B	Technical Diagram of IRFZ44N MOSFET	145
Appendix C	Technical Diagram of the IR2104 MOSFET Driver	148
Appendix D	Anatomy of Arduino UNO Pin Functions	150
Appendix E	Current Sensor ACS217	150
Appendix F	Test Load for Testing	151
Appendix G	Charge Controller MPPT Program	151
Appendix H	LCD and Data Logger	163
Appendix I	Results Data	169

# CHAPTER 1

## INTRODUCTION

### 1.1 Research Background

Concerns about global warming, climate change, rising greenhouse gas emissions, and energy resource depletion have resulted in a greater understanding of how resources can be used most efficiently. Peninsular Malaysia's peak electricity demand was 15,476 Mega Watts (MW) in May 2011 and is expected to reach 21 Giga Watts (GW) in 2020. Furthermore, among other renewable energy options, the use of solar photovoltaic (PV) with a capacity potential of up to 6,500 MW in the country's energy mix has been identified as having the highest capacity potential (Yow, et al., 2011). Nonetheless, as is true throughout the world, the use of solar photovoltaic is the solution for telecommunications organisations such as France Telecom and Vodafone, which are the main players in potential green telecommunications and Integrated Circuit (IC) services (Lubritto, 2012).

Therefore, the solution to the need for reliable off-grid power is to use solar PV. Stand-alone solar PV systems, for example, are commonly used for off-grid power applications such as rural lighting, telecommunication base stations, and remote monitoring. This stand-alone power option is currently being considered for a Fiber Wireless (FiWi) system based on Radio-over-Fiber (RoF) technology.

The base stations of the FiWi system or Remote Antenna Unit (RAU) will be installed in remote or blind-spot urban areas where grid-connected power supplies are not available or where construction or wall hacking is unacceptable. As such, the use of a stand-alone PV system would be appropriate. Wireless signals in RoF systems are transmitted optically between a Central Station (CS) and a Base Terminal Station (BTS) set or a RAU before being radiated through the air. The base

station is designed to communicate within the base station's radio range via a radio link.

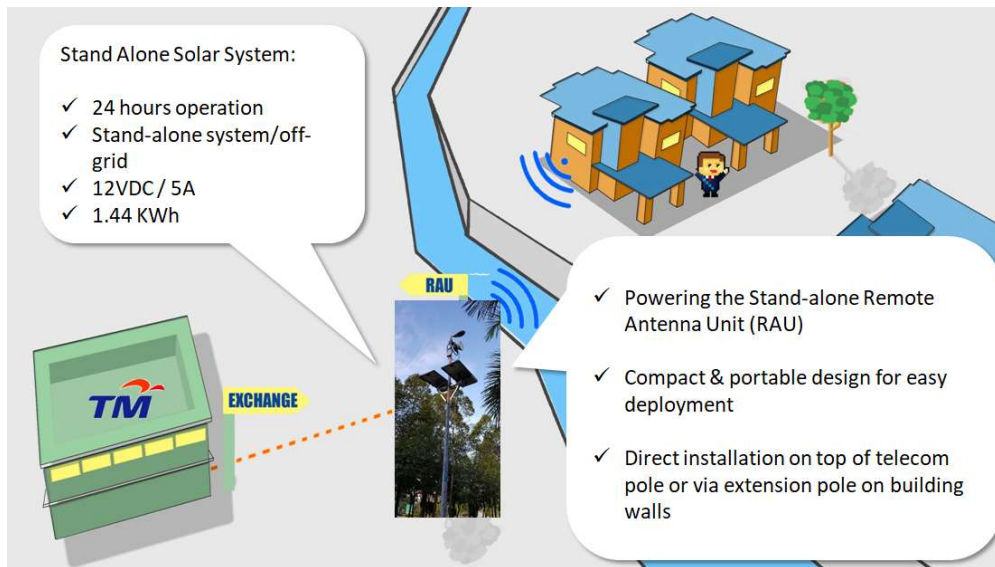


Figure 1.1 Overall FiWi system based on RoF deployment

Part of the work requirement is to support the power supply of the RoF RAU using renewable power sources. This is achieved by developing a PV system with smart power management, which controls the power distribution and energy saving functions for the system. Figure 1.1 shows the overall FiWi system based on RoF deployment.

A compact PV power unit is a system which uses PV to convert sunlight into electricity, which is then stored in a battery and controlled by the battery management system. It consists of multiple components such as photovoltaic modules, charge controller, battery, mechanical and electrical connections, mountings, and a voltage regulator as a means of regulating and modifying the electrical output as required by the load.

The system itself is a portable power supply unit which enables it to provide internet access and communication in areas and situations where power is non-existent, unreliable or as an alternative to the electric grid. The smart power management manages the power consumption between the solar panel, the battery

and the RAU. The system monitors the charging of the battery and the RAU power consumption for the reliability and performance of the system.

This research will deliver the compact PV system for further integration as a power source for the deployment of the RoF RAU for outdoor usage. This research will focus on the design, development, and integration of the PV system with the power management.

## **1.2 Problem Statement**

Variations in weather conditions have a significant impact on the power efficiency and performance of a PV system. The amount and temperature of available sunlight have an impact on the performance of photovoltaic systems. The amount of light that reaches the photovoltaic cell is reduced by shading. Furthermore, the temperature is affected by the mounting materials and design of the photovoltaic system. The goal is to use an algorithm to determine the Maximum Power Point Tracking (MPPT). The MPPT methods and the difficulties in tracking them in rapidly changing environmental conditions. According to new research, the majority of Maximum Power Point (MPP) trackers used Perturbation and Observation (P&O) and Incremental Conductance (INC) techniques and tracked in the wrong direction when environmental conditions changed quickly. Because the output of the photovoltaic system is dependent on irradiation, temperature, and the electrical characteristics of the load, it may be unable to deliver the output voltage perfectly. Weather changes cause changes in irradiance and temperature, which can have a significant impact on the power efficiency and performance of PV systems.

Variations in the values of PV system parameters such as the PV voltage or the load influence the overshoot voltage and oscillation around MPP. The MPP's response is slow, and it loses track of its overshoot voltage condition. Because of these disadvantages, an efficient design of a photovoltaic system is necessary. MPPT is a well-established algorithm in PV applications for extracting the maximum



amount of energy possible from the photovoltaic panel to maximize power transfer under all operating conditions.

The improved algorithm is the primary solution that regulates Pulse Width Modulation (PWM) by adjusting the duty cycle  $D$  and step size. In the traditional fixed step size in the P&O method, there is a trade-off between tracking speed and tracking precision. As small step sizes are used, the procedure eventually converges on the MPP. When a large step size is used, it results in device power losses due to photovoltaic power oscillations around the MPP. When the weather changes, the operating point should be moved away from the MPP. To overcome all of the fixed step size's disadvantages, a variable step size MPPT is required to achieve adequate tracking precision and speed while retaining the benefit of easy calculation. When the working point is a long distance from the MPP, the search process will take a large step. However, when the working point is close to the MPP, the search step will automatically change to a tiny one. It is possible to minimize both the search time and the overshoot voltage. A variable step MPPT method is used for a faster and more precise tracking process.

Typically, a PV panel generates approximately 17 V for a 60 W panel and limits maximum power output to a few hours per day of 12 V battery charging. A PWM that controls the Direct Current to Direct Current (DC-DC) buck converter is installed between the PV and batteries to address this issue. Although the panel voltage of a buck converter is higher than the battery voltage, the DC-DC buck converter has a method for rectifying this situation. The buck converter is one of the fundamental topologies of DC-DC converters operating in switched-mode, capable of producing any output voltage according to the fundamental topologies. This research proposes a DC-DC buck converter circuit with an MPPT algorithm that can be simulated with any irradiance reading to demonstrate the effect of irradiance on the photovoltaic output. The DC-DC converter and algorithm method can help reduce the oscillation and settling time during the maximum point acquisition process and improve converter performance.

### **1.3 Research Objectives**

The primary goal of this thesis is to conduct research on Perturbation and Observation (P&O) MPPT and improve the method of implementing MPPT algorithms in a software program for DC-DC converter hardware. Modelling of the solar cell and the DC-DC converter using MATLAB/Simulink<sup>®</sup> and interfacing them together in one system with the MPPT algorithm to obtain the maximum power point operation would be of most importance. This objective can be achieved through the following specific goals:-

- a) To propose an MPPT algorithm by improving P&O with a variable step size for PV systems to reach MPPT more quickly and efficiently in varying weather conditions. To reduce overshoot voltage and oscillation around MPP and eliminate the loss of tracking.
- b) To reduce overshoot voltage and oscillation around MPP and eliminate the loss of tracking.
- c) To design and fabricate a DC-DC buck converter with an adjustable step size in the MPPT algorithm. Improve the performance of the DC-DC buck converter by monitoring the output voltage close to its reference value, which should give excellent accuracy to the DC-DC converter.
- d) To validate the proposed MPPT algorithm and DC-DC converter through simulation and experiments.

### **1.4 Strategy of Research**

The main purpose of this work is to analyze and examine the PV system's power efficiency and performance under changing weather conditions and loads through improved MPPT algorithms and converters. The following activities are included in the scope of the work to achieve the main goal and specific goals of this project.

- a) Simulate the characteristics of a solar cell. Measure the voltage, current, power, and compare between the simulation and measurement.
- b) Design a DC-DC converter and improve the MPPT algorithm by introducing a P&O algorithm with a variable step size.
- c) A vindication by simulating the characteristics of the proposed DC-DC converter.
- d) The final step is to conduct an experiment to measure the panel system and power accuracy as well as the performance of the photovoltaic system.

The main task is to perform the simulation using MATLAB/Simulink<sup>®</sup>. The PV cell concept and its characteristics have been studied and obtained through its characteristic equation using the SimScape to solve the diode equation.

The converter model is implemented with the SimPower and System Block Set based on computer simulation using the MATLAB/Simulink<sup>®</sup> software. In designing, testing, and assessing the power electronic converter and its components, computer simulation plays an important role. MATLAB/Simulink<sup>®</sup> is a powerful tool for testing all PV systems. The benefits of using MATLAB/Simulink<sup>®</sup> are its quicker response, availability of different simulation methods and usable blocks, and lack of convergence issues.

The next task is to assemble all the PV components, which are the 60W PV from SolarTIF Sdn Bhd, Model TIF60W, Maximum Power Point Tracking (MPPT) converter, test load and 120 Ah 12 V LiFePO<sub>4</sub> battery. The testing and measurement of power accuracy and the performance of the PV system will be conducted in the laboratory.

The third task is to analyze the results obtained from the experimental work. This task also includes a detailed discussion of the analysis. Finally, in the conclusion, the key results of this research are summarized to present the

contribution of the analysis given to the goals of the research. Figure 1.2 demonstrates the methodology of the research.

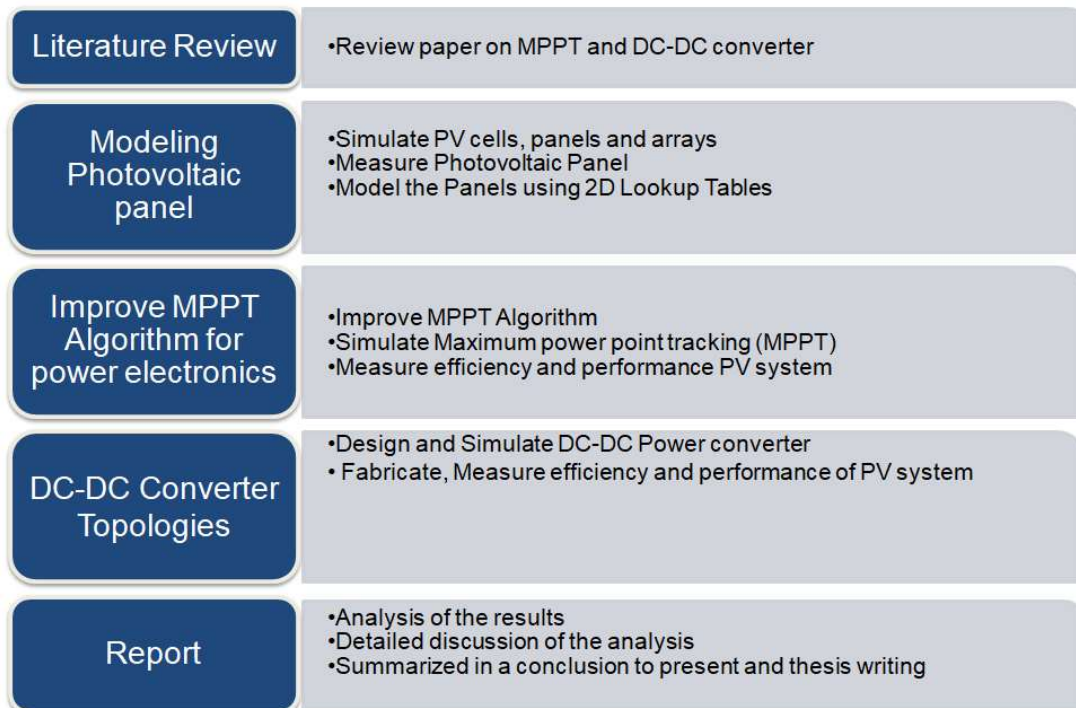


Figure 1.2 Research methodology

## 1.5 Outline of Thesis

This thesis is divided into five chapters. The first chapter describes PV system technology and its applications in telecommunications. It also includes a definition of the issue as well as the research's aims, purpose, and scope. The second chapter provides an overview of the research's theoretical history, photovoltaic cell theory, DC-DC converter theory, and the MPPT Algorithm. It goes over a variety of PV-related issues. The third chapter provides an overview and description of the analysis, its components, methods, and detailed procedures. The fourth chapter examines the results of the experimental studies. It also addresses the PV system's accuracy and performance tests. The final chapter, Chapter 5, describes the findings and recommendations of this future research.

## REFERENCES

- Abdulkadir, M., Samosir, A. S. and Yatim, A. H. M. (2012) 'Modeling and Simulation Based Approach of Photovoltaic System in Simulink Model', *ARPN Journal of Engineering and Applied Sciences* Vol. 7, no. 5, May 2012, ISSN 1819-6608.
- Ahmed, J., and Salam, Z. (2013) 'A Soft Computing MPPT for PV System Based on Cuckoo Search Algorithm', *4th International Conference on Power Engineering, Energy and Electrical Drives*, Istanbul, Turkey. 13-17 May 2013, 558-562.
- Ahmed, J., and Salam, Z. (2016) 'A Modified P&O Maximum Power Point Tracking Method With Reduced Steady-State Oscillation and Improved Tracking Efficiency IEEE Transactions on Sustainable Energy', Vol. 7, No. 4, Oct 2016. 1506-1515.
- Alajmi, B. N., Ahmed, K. H., Adam, G. P. and Williams, B. W. (2013) 'Single-Phase Single-Stage Transformer less', *IEEE Transactions on Power Electronics*, 28(6), 2664–2676.
- Algazar, M., Hamdy, A., Hamdy, A. E., Mohamed Ezzat El, K. S. (2012) 'Maximum power point tracking using fuzzy logic control', *Electrical Power and Energy Systems* 39 21–28.
- Andrejas, T. (2011) 'Comparison of direct maximum power point tracking algorithms using EN 50530 dynamic test procedure', *IET Renew. Power Gener.*, 5(4), 281–286.
- Banu, I. V. and Istrate, M. (2012). Modeling of maximum power point tracking algorithm for photovoltaic systems. *2012 International Conference and Exposition on Electrical and Power Engineering*. (2): 953–957.
- Barca, G., Moschetto, A., Sapuppo, C., Tina, G. M., Giusto, R., and Grasso, A. D. (2008). A novel MPPT charge regulator for a photovoltaic stand-alone telecommunication system. *2008 International Symposium on Power Electronics, Electrical Drives, Automation and Motion*. : 235–238.
- Boualem Bendib, Hocine Belmili and Fateh Krim (2015) 'A survey of the most used MPPT methods: Conventional and advanced algorithms applied for

- photovoltaic systems', *Renewable and Sustainable Energy Reviews* 45 (2015), 637–648
- Bouilouta, A., Mellit, A. and Kalogirou, S.A. (2013) 'New MPPT method for standalone photovoltaic systems operating under partially shaded conditions', *Energy*, 55, 1172–1185.
- Bouzelata, Y., Kurt E., Altın, N. and Chenni, R. (2015) 'Design and simulation of a solar supplied multifunctional active power filter and a comparative study on the current detection algorithms', *Renewable and Sustainable Energy Reviews*, 43, 1114–1126.
- Brito, M. A. G., Galotto, L. Jr., Sampaio, L. P., Melo, G. de A. e, and Canesin, C. A. (2013) 'Evaluation of the Main MPPT Techniques for Photovoltaic Applications', *IEEE Transactions on Industrial Electronics*, 60(3)1156–1167.
- Chen, P., Chen, P. Y., Liu, Y. H., Chen, J. H., Luo, Y. F. (2015) 'A comparative study on maximum power point tracking techniques for photovoltaic generation systems operating under fast changing environments', *Science Direct, Solar Energy*, 119 (2015) 261–276.
- Chen, Y., Jhang, Y. and Liang, R. (2016) 'A Fuzzy-Logic Based Auto-Scaling Variable Step-Size MPPT Method for PV Systems', *Solar Energy*, 126, 53–63. 140
- Das, A. K. (2011) 'An explicit J-V model of a solar cell for simple fill factor calculation', *Sol. Energy*, 85(9): 1906-1909.
- Dasgupta, N., Pandey, A. and Mukerjee, A. K. (2008) Voltage-sensing-based photovoltaic MPPT with improved tracking and drift avoidance capabilities', *Solar Energy Materials & Solar Cells*, 92, 1552–1558.
- Dileep, G. and Singhb, S.N. (2017) 'Selection of non-isolated DC-DC converters for solar photovoltaic', *System Renewable and Sustainable Energy Reviews* 76 (2017) 1230–1247
- Engin, M. B. and Bekir, C. (2016) 'Comparisons of MPPT performances of isolated and non-isolated DC–DC converters by using a new approach', *Renewable and Sustainable Energy Reviews* 60, 1100–1113.
- Femia, N., Petrone, G., Spagnuolo, G. and Vitelli M. (2005) 'Optimization of Perturb and Observe Maximum Power Point Tracking Method', *IEEE*

*Transactions on Power Electronics, Vol. 20, NO. 4, July 2005 963.*

- Foo Y. C., Hudi N. S. and Kuan T. M. (2019) 'Insight into the Trending of Solar Radiation and Ambient Temperature in Malaysia towards a Possible Implementation on Step-Wise Rating', *CIGRE-IEC 2019 Conference on EHV and UHV (AC & DC)*, 1-13.
- Fu, C. and Su, S. (2011) 'Simulation Studying of MPPT Control by a New Method for Photovoltaic Power System', *Electrical and Control Engineering (ICECE), 2011 International Conference*, 1274–1278.
- Ghassami, A. A., Sadeghzadeh, S. M., and Soleimani, A. (2013) 'Electrical Power and Energy Systems A high performance maximum power point tracker for PV systems', *International Journal of Electrical Power and Energy Systems*, 53, 237–243.
- Husna A.W. N., Siraj, S.F. and Ab Muin, M. Z. (2012). 'Modeling of DC-DC converter for solar energy system applications', *2012 IEEE Symposium on Computers & Informatics (ISCI)*. : 125–129.
- Irmak, E., and Naki, G. (2013) 'Application of a high efficient voltage regulation system with MPPT algorithm', *Electronic Power Energy System*, 44, 703–712.
- Ishaque, K., Salam Z. (2013) 'A review of maximum power point tracking techniques of PV system for uniform insolation and partial shading condition', *Renewable and Sustainable Energy Reviews* 19 (2013), 475–488.
- Jantsch M., Real M., Häberlin H., Whitaker C., Kurokawa K., Blässer G., Kremer P., Verhoeve C.W.G. (2016) 'Measurement of PV Maximum Power Tracking Performance', *International Electrotechnical Commission*.
- Jiang, J. A., Huang, T. L., Hsiao, Y. T. and Chen. C. H. (2005) 'Maximum Power Tracking for Photovoltaic Power Systems', *Journal of Science and Engineering*, Vol. 8, No 2, pp. 147153 (2005)
- Jiang, J. Su, Y. Shieh, J., Kuo, K., Lin, T., Lin, T., Fang, W., Chou, J. and Wang, J. (2014) 'On application of a new hybrid maximum power point tracking (MPPT) based photovoltaic system to the closed plant factory', *Applied Energy*. 124, 309–324.
- Jiang, Y., Jaber, A. Q. A., and Tim, A. H. (2013) 'Adaptive Step Size With Adaptive-Perturbation- Frequency Digital MPPT Controller for a Single-

- Sensor Photovoltaic Solar System', *IEEE Transactions on Power Electronics*, Vol 28, NO. 7, JULY 2013
- Kakosimos, P. E. and Kladas, A. G. (2011) 'Implementation of photovoltaic array MPPT through fixed step predictive control technique', *Renewable Energy*, 36(9), 2508–2514.
- Karanjkar, D. S., Chatterji, S., Kumar, A. and Shimi, S. L. (2014) 'An Open Fuzzy adaptive proportional integral derivative controller with dynamic set-point adjustment for maximum power point tracking in solar photovoltaic system', *Systems Science & Control Engineering*, 2(1), 562-582.
- Kasbi, S., and Rijanto, E. (2015) 'Design And Implementation Of Controller For Boost DC-DC Converter Using PI-LPF Based on Small Signal Model', *Journal of Mechatronics, Electrical Power*, 06, 105–112.
- Khazaei, J. Piyasinghe, L., Miao, Z. and Fan L. (2015) 'Real-Time Digital Simulation-Based Modeling of A Single- Phase Single-Stage PV System', *Electric Power Systems Research*, 123, 85– 91.
- Kheldoun, Bradai, A. R., Boukenoui, R. and Mellit, A. (2016) 'A new Golden Section method-based maximum power point tracking algorithm for photovoltaic systems', *Energy Conversion and Management*, 111, 125–136.
- Khemiri, N., Khedher, A., and Mimouni, M. F. (2013). 'A sliding mode control approach applied to a photovoltaic system operated in MPPT', *10th International Multi-Conferences on Systems, Signals & Devices*. : 1–6.
- Koutroulis, Eftichios, Kostas Kalaitzakis, and Nicholas C. Voulgaris (2001) 'Development of a Microcontroller-Based, Photovoltaic Maximum Power Point Tracking Control System', *IEEE Transaction Sun Power Electronics*, Vol.16, NO.1, January 2001
- Lalili, D. (2013) 'State feedback control and variable step size MPPT algorithm of three-level grid-connected photovoltaic inverter', *Solar Energy*, 98,561– 571.
- Li, X., Wen H., Hu Y. (2016) 'Evaluation of Different Maximum Power Point Tracking (MPPT) Techniques based on Practical Meteorological Data', *International Conference on renewable Energy Research and Applications*, Nov 2016
- Liu, F. Duan, S., Liu, F., Liu, B. and Kang, Y. (2008) 'A variable step size inc MPPT method for PV systems', *IEEE Trans. on industrial electronics*, 55(7),



2622-2628.

- Liu, Y. Li, M., Ji X., Luo, X., Wang, M., and Zhang Y. (2014) 'A comparative study of the maximum power point tracking methods for PV systems', *Energy Conversion and Management*, 85, 809–816.
- Lubritto, C. (2012) 'Telecommunication Power System: Energy Saving, Renewable Sources and Environmental Monitoring', Trends in Telecommunications Technologies. *Christos J Bouras (Ed.), InTech*, 30/11/2012
- Mastromauro, R. A., Liserre, M., Member, S., and Aquila, A. D. (2012) 'Control Issues in Single-Stage Photovoltaic Systems: MPPT', *Current and Voltage Control*, 8(2), 241–254.
- Mei, Q., Shan, M., Liu, L. and Guerrero, M. J. (2011) 'A Novel Improved Variable Step-Size Method for PV Systems', *IEEE Transactions on Industrial Electronics*, 58(6), 2427–2434.
- Mellit, A., Rezzouk, H., Messai, A., and Medjahed, B. (2011) 'FPGA-based real time implementation of MPPT-controller for photovoltaic systems', *Renewable Energy*, 36(5), 1652–1661.
- Mirbagheri, S. Z., Mekhilef, S. and Mirhassani, S. M. (2013) 'MPPT with Inc. Cond method using conventional interleaved boost converter', *Energy Procedia*, 42, 24–32.
- Mohammed, A. E., Zahawi, B. and David J. A. (2012). 'Assessment of Perturb and Observe MPPT Algorithm Implementation Techniques for PV Pumping', Applications. *IEEE Transactions on Sustainable Energy*. 3(1) :21-33
- Nabil, K., Moubayed, N., Outbib, R. (2017) 'General review and classification of different MPPT Techniques', *Renewable and Sustainable Energy Reviews*, 68 (2017) 1–18.
- Nabulsi, A. Al, and Dhaouadi, R. (2012) 'Efficiency Optimization of a DSP-Based Standalone PV System Using Fuzzy Logic and Dual-MPPT Control', *IEEE Transactions on Industrial Informatics*, 8(3), 573–584.
- Ozdemir, S., Altin, N. and Sefa, I. (2014) 'Single stage three level grid interactive MPPT inverter for PV systems', *Energy Conversion and Management*, 80, 561–572.
- Pandiarajan, N., and Muthu, R. (2011) 'Development of Power Electronic Circuit-oriented Model of Photovoltaic Module', *International Journal of Advanced*

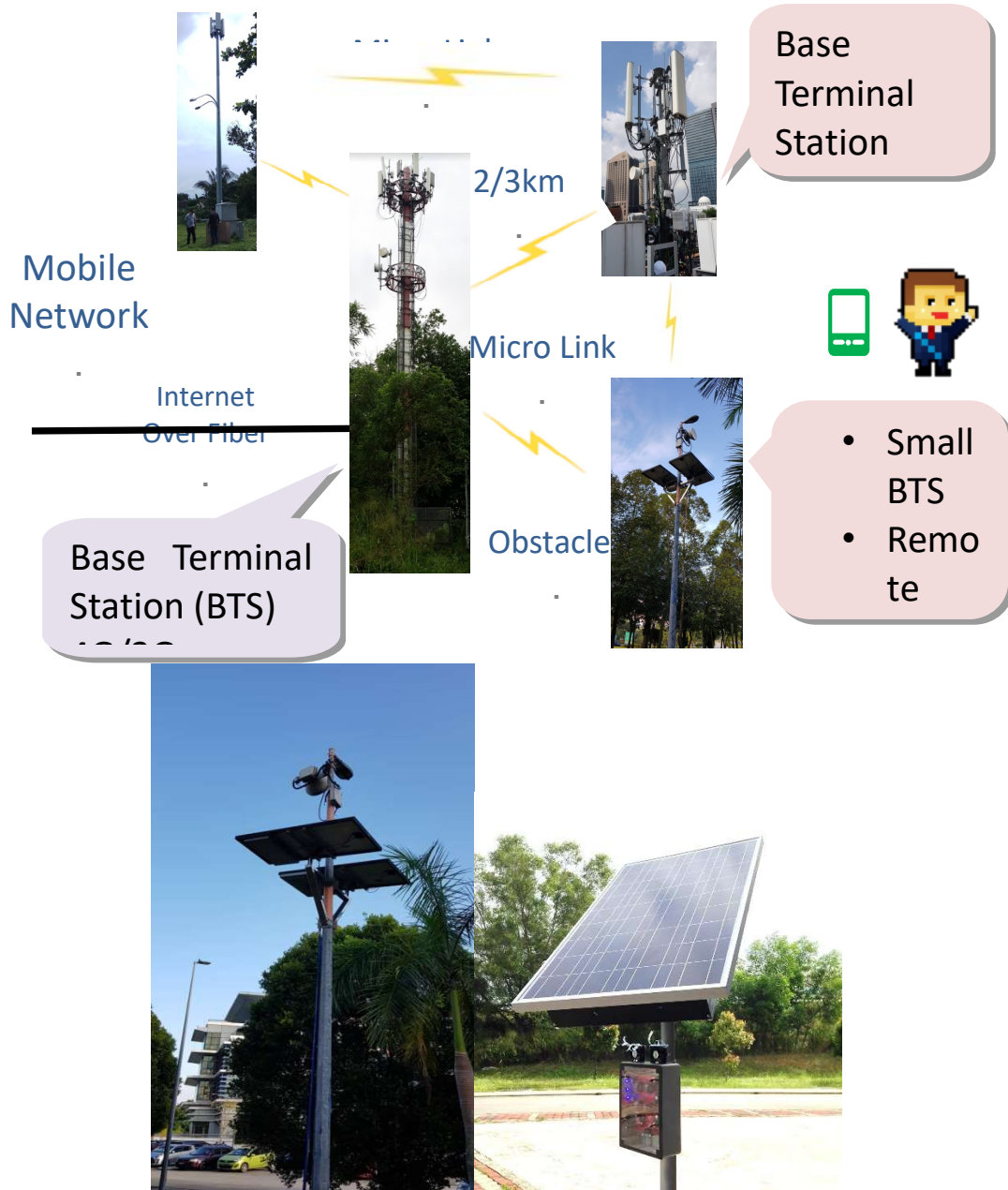
*Engineering Technology*, E-ISSN 0976-3945, 2011.

- Pandiarajan, N., Ramaprabha, R. and Ranganath M. (2008) 'Circuit Modeling Process for Photovoltaic Module', *Application of Circuit Model for Photovoltaic Energy Conversion System*. Volume 2012 |Article ID 410401.
- Ping, W., Hui, D., Changyu, D., and Shengbiao, Q. (2011) 'An Improved MPPT Algorithm Based on Traditional Incremental Conductance Method', *2011 4th International Conference on Power Electronics Systems and Applications*. (2): 1–4.
- Prasad, Y., Chhetri, B. B., Adhikary, B., and Bista, D. (2010) 'Microcontroller Based Intelligent Dc/Dc Converter To Track Maximum Power Point', *IEEE*, 94–101.
- Punitha, K., Devaraj, D. and Sakthivel, S. (2013) 'Artificial neural network based modified incremental conductance algorithm for maximum power point tracking in photovoltaic system under partial shading conditions', *Energy*, 62(3), 30–40.
- Radjai, T. Rahmani, L., Mekhilef, S., and Gaubert, J. P. (2014) 'Implementation of a modified incremental conductance MPPT algorithm with direct control based on a fuzzy duty cycle change estimator using dSPACE', *Solar Energy*, 110, 325–337.
- Salas, V. A., Olias, E., Barrado, A. and Lazaro, A. (2006) 'Review of the maximum power point tracking algorithms for stand-alone photovoltaic systems', *Solar Energy Materials & Solar Cells*, 90, 1555–1578.
- Salmi, T., Bouzguenda M., Gastli A. and Masmoudi A. (2012) 'MATLAB/Simulink Based Modelling of Solar Photovoltaic Cell', *International Journal of Renewable Energy Research*. 2(2):213-218.
- Sharma, D. K. and Purohit, G. (2012) 'Advanced Perturbation and Observation (P&O) based Maximum Power Point Tracking (MPPT) of a Solar Photovoltaic System', *Power Electronics (IICPE), 2012 IEEE 5th India International Conference on*, (Delhi). 3(7).
- Sheng, S. and Lehman B. (2016) 'A Simple Variable Step Size Method for Maximum Power Point Tracking Using Commercial Current Mode Control DC-DC Regulators', *2016 IEEE Applied Power Electronics Conference and Exposition (APEC)*. Electronic ISBN: 978-1-4673-9550-2.

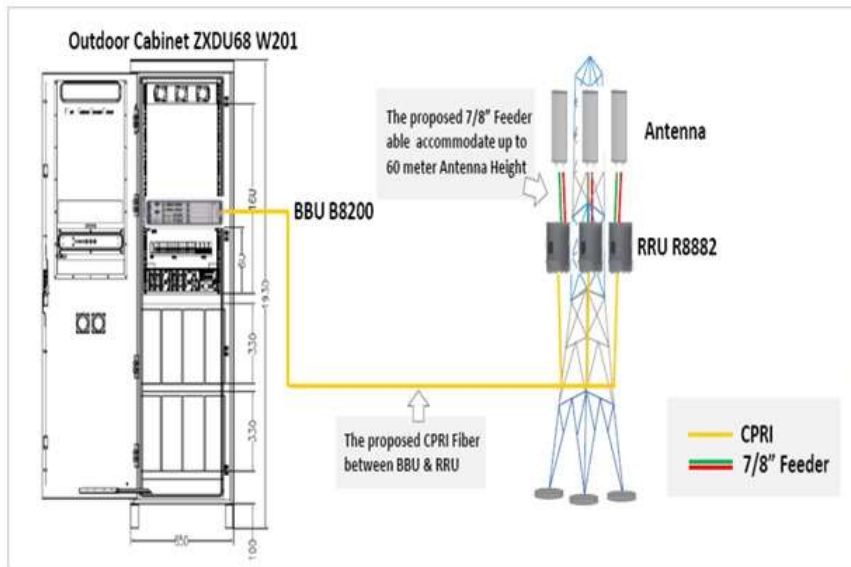
- Sun, C. and Wang Y. (2016) 'Research of kind of variable step size perturbation and observation MPPT based on power prediction', *Proceedings of 2016 IEEE International Conference on Mechatronics and Automation* August, 7 – 10.
- Tafticht, T., Agbossou, K., Doumbia, M. L, Cheriti, A. (2008) 'An improved maximum power point tracking method for photovoltaic systems', *Renewable Energy*, 33 (2008) 1508–1516.
- Tey, K. S. and Mekhilef, S. (2014) 'Science Direct Modified incremental conductance MPPT algorithm to mitigate inaccurate responses under fast changing solar irradiation level', *Solar Energy*, 101, 333–342.
- Tey, K. S. and Mekhilef, S., (2013) 'A Fast converging MPPT Technique for Photovoltaic System under Fast Varying Solar Irradiation and Load Resistance', *IEEE Transaction on Industrial Informatics*, 1551-3203.
- Tsai, H. L., Tu, C. S., and Su Y. J. (2008) 'Development of Generalized Photovoltaic Model Using MATLAB/SIMULINK', *Proceedings of the World Congress on Engineering and Computer Science*, ISBN: 978-988-98671-0-2.
- Vivek, P., Ayshwarya R. S., Amali J., Sree A.S.N. (2016) 'A Novel Approach on MPPT Algorithm for Solar Panel using Buck Boost Converter', *2016 International Conference on Energy Efficient Technologies for Sustainability (ICEETS)*, Electronic ISBN:978-1-4673-9925-8.
- Wang, J. C., Ding, L. and Li, N. (2011) 'High-accuracy maximum power point for photovoltaic arrays', *Sol Energy Mater Sol Cells*, 95, 843–51.
- Yaden, M. F., Ouariachi, M. El, and Chadli, E. L. (2011). 'Design and Realization of a Photovoltaic System Equipped with a Digital MPPT Control', *Multimedia Computing and Systems (ICMCS), 2011 International Conference*, (978-1-61284-730-6), 1 – 6.
- Yan, Z. Fei, L., Jinjun, Y. and Shanxu D. (2008) 'Study on Realizing MPPT by Improved Incremental Conductance Method with Variable Step-size', *IEEE*, 547–550.
- Yow, P. L., Mustapha, S. I. and Hashim A. H. (2011) 'Climate Change Challenges on CO<sub>2</sub> Emission Reduction for Developing Countries: A Case for Malaysia's Agenda for Action', *The International Journal of Climate Change: Impacts and Responses*, 2.

## Appendix A Actual Equipment

A Actual Load



# Outdoor Equipment Cabinet to Tower



14

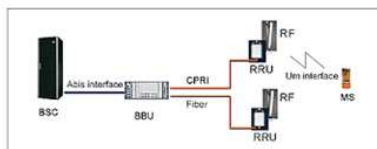


Fig. 1 BBU-RRU structure

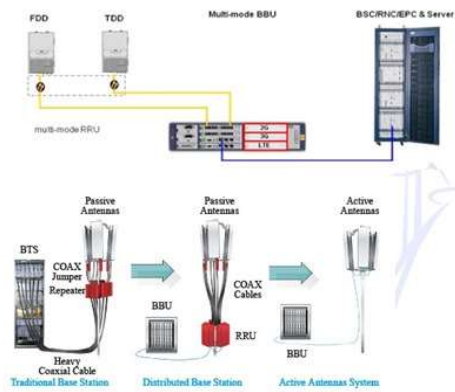
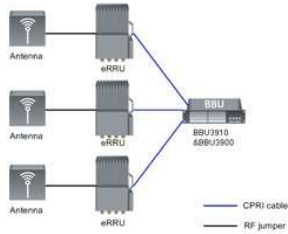


Figure 1. Development of base station architecture.

## Appendix B Technical Diagram of IRFZ44N MOSFET

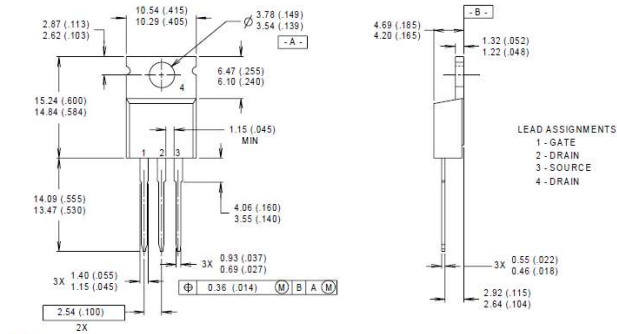
IRFZ44N

International  
IR Rectifier

Package Outline

TO-220AB

Dimensions are shown in millimeters (inches)

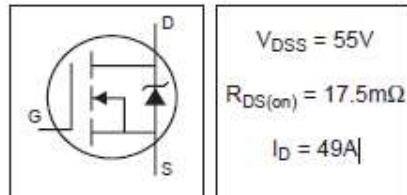


- NOTES:
- 1 DIMENSIONING & TOLERANCING PER ANSI Y14.5M, 1992.
  - 2 CONTROLLING DIMENSION : INCH
  - 3 OUTLINE CONFORMS TO JEDEC OUTLINE TO-220AB.
  - 4 HEATSINK & LEAD MEASUREMENTS DO NOT INCLUDE BURRS.

# IRFZ44N

HEXFET® Power MOSFET

- Advanced Process Technology
- Ultra Low On-Resistance
- Dynamic dv/dt Rating
- 175°C Operating Temperature
- Fast Switching
- Fully Avalanche Rated



### Description

Advanced HEXFET® Power MOSFETs from International Rectifier utilize advanced processing techniques to achieve extremely low on-resistance per silicon area. This benefit, combined with the fast switching speed and ruggedized device design that HEXFET power MOSFETs are well known for, provides the designer with an extremely efficient and reliable device for use in a wide variety of applications.

The TO-220 package is universally preferred for all commercial-industrial applications at power dissipation levels to approximately 50 watts. The low thermal resistance and low package cost of the TO-220 contribute to its wide acceptance throughout the industry.



### Absolute Maximum Ratings

	Parameter	Max.	Units
$I_D @ T_C = 25^\circ C$	Continuous Drain Current, $V_{GS} @ 10V$	49	A
$I_D @ T_C = 100^\circ C$	Continuous Drain Current, $V_{GS} @ 10V$	35	
$I_{DM}$	Pulsed Drain Current ①	160	
$P_{tot} @ T_C = 25^\circ C$	Power Dissipation	94	W
	Linear Derating Factor	0.63	W/°C
$V_{GS}$	Gate-to-Source Voltage	$\pm 20$	V
$I_{AR}$	Avalanche Current ②	25	A
$E_{AS}$	Repetitive Avalanche Energy ③	9.4	mJ
dv/dt	Peak Diode Recovery dv/dt ④	5.0	V/ns
$T_J$	Operating Junction and	-55 to +175	°C
$T_{STG}$	Storage Temperature Range		
	Soldering Temperature, for 10 seconds	300 (1.6mm from case )	
	Mounting torque, 6-32 or M3 screw	10 lbf-in (1.1N-m)	

### Thermal Resistance

	Parameter	Typ.	Max.	Units
$R_{\theta JC}$	Junction-to-Case	—	1.5	°C/W
$R_{\theta CS}$	Case-to-Sink, Flat, Greased Surface	0.50	—	
$R_{\theta JA}$	Junction-to-Ambient	—	62	



## Electrical Characteristics @ $T_J = 25^\circ\text{C}$ (unless otherwise specified)

	Parameter	Min.	Typ.	Max.	Units	Conditions
$V_{(BR)DSS}$	Drain-to-Source Breakdown Voltage	55	—	—	V	$V_{GS} = 0V, I_D = 250\mu A$
$\Delta V_{(BR)DSS}/\Delta T_J$	Breakdown Voltage Temp. Coefficient	—	0.058	—	V/°C	Reference to $25^\circ\text{C}, I_D = 1\text{mA}$
$R_{DS(on)}$	Static Drain-to-Source On-Resistance	—	—	17.5	mΩ	$V_{GS} = 10V, I_D = 25A$ ④
$V_{GS(th)}$	Gate Threshold Voltage	2.0	—	4.0	V	$V_{DS} = V_{GS}, I_D = 250\mu A$
$g_m$	Forward Transconductance	19	—	—	S	$V_{DS} = 25V, I_D = 25A$ ④
$I_{DSS}$	Drain-to-Source Leakage Current	—	—	25	μA	$V_{GS} = 55V, V_{DS} = 0V$ $V_{DS} = 44V, V_{GS} = 0V, T_J = 150^\circ\text{C}$
$I_{OSS}$	Gate-to-Source Forward Leakage	—	—	100	nA	$V_{DS} = 20V$
	Gate-to-Source Reverse Leakage	—	—	-100	nA	$V_{DS} = -20V$
$Q_{gT}$	Total Gate Charge	—	—	63	nC	$I_D = 25A$
$Q_{gs}$	Gate-to-Source Charge	—	—	14	nC	$V_{DS} = 44V$
$Q_{gd}$	Gate-to-Drain ("Miller") Charge	—	—	23	nC	$V_{DS} = 10V$ , See Fig. 6 and 13
$t_{d(on)}$	Turn-On Delay Time	—	12	—	ns	$V_{DD} = 26V$
$t_r$	Rise Time	—	60	—	ns	$I_D = 25A$
$t_{d(off)}$	Turn-Off Delay Time	—	44	—	ns	$R_{\theta} = 12\Omega$
$t_f$	Fall Time	—	45	—	ns	$V_{GS} = 10V$ , See Fig. 10 ④
$L_D$	Internal Drain Inductance	—	4.5	—	nH	Between lead, 6mm (0.25in.) from package and center of die contact
$L_S$	Internal Source Inductance	—	7.5	—	nH	
$C_{iss}$	Input Capacitance	—	1470	—	pF	$V_{DS} = 0V$
$C_{oss}$	Output Capacitance	—	360	—	pF	$V_{DS} = 25V$
$C_{riss}$	Reverse Transfer Capacitance	—	88	—	pF	$f = 1.0\text{MHz}$ , See Fig. 5
$E_{AS}$	Single Pulse Avalanche Energy ②	—	5300	1500	mJ	$I_{AS} = 25A, L = 0.47\text{mH}$

## Source-Drain Ratings and Characteristics

	Parameter	Min.	Typ.	Max.	Units	Conditions
$I_S$	Continuous Source Current (Body Diode)	—	—	49	A	MOSFET symbol showing the integral reverse p-n junction diode.
$I_{SM}$	Pulsed Source Current (Body Diode) ①	—	—	160	A	
$V_{SD}$	Diode Forward Voltage	—	—	1.3	V	$T_J = 25^\circ\text{C}, I_S = 25A, V_{GS} = 0V$ ④
$t_{rr}$	Reverse Recovery Time	—	63	95	ns	$T_J = 25^\circ\text{C}, I_F = 25A$
$Q_{rr}$	Reverse Recovery Charge	—	170	260	nC	$di/dt = 100A/\mu s$ ④
$t_{on}$	Forward Turn-On Time	Intrinsic turn-on time is negligible (turn-on is dominated by $L_S+L_D$ )				

### Notes:

① Repetitive rating; pulse width limited by max. junction temperature. (See fig. 11)

② Starting  $T_J = 25^\circ\text{C}$ ,  $L = 0.48\text{mH}$   
 $R_{\theta} = 25\Omega$ ,  $I_{AS} = 25A$ . (See Figure 12)

③  $I_{SD} \leq 25A$ ,  $di/dt \leq 230A/\mu s$ ,  $V_{DD} \leq V_{(BR)DSS}$ ,  
 $T_J \leq 175^\circ\text{C}$

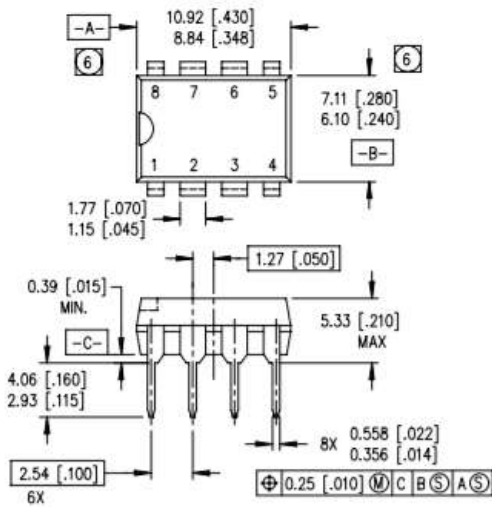
④ Pulse width  $\leq 400\mu s$ ; duty cycle  $\leq 2\%$ .

⑤ This is a typical value at device destruction and represents operation outside rated limits.

⑥ This is a calculated value limited to  $T_J = 175^\circ\text{C}$ .

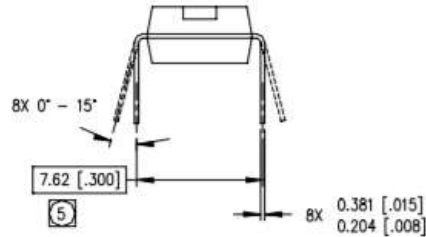


## Appendix C Technical Diagram of the IR2104 MOSFET Driver



### NOTES:

1. DIMENSIONING & TOLERANCING PER ANSI Y14.5M-1982.
2. CONTROLLING DIMENSION: INCH.
3. DIMENSIONS ARE SHOWN IN MILLIMETERS [INCHES].
4. OUTLINE CONFORMS TO JEDEC OUTLINE MS-001AB.
5. MEASURED WITH THE LEADS CONSTRAINED TO BE PERPENDICULAR TO DATUM PLANE C.
6. DIMENSION DOES NOT INCLUDE MOLD PROTRUSIONS. MOLD PROTRUSIONS SHALL NOT EXCEED 0.25 [.010].



8 Lead PDIP

01-6014  
01-3003 01 (MS-001AB)

International  
**IR** Rectifier

Data Sheet No. PD60046-Q

**IR2104(S)**

**HALF-BRIDGE DRIVER**

### Features

- Floating channel designed for bootstrap operation Fully operational to +600V Tolerant to negative transient voltage dV/dt immune
- Gate drive supply range from 10 to 20V
- Undervoltage lockout
- 3.3V, 5V and 15V input logic compatible
- Cross-conduction prevention logic
- Internally set deadtime
- High side output in phase with input
- Shut down input turns off both channels
- Matched propagation delay for both channels

### Description

The IR2104(S) are high voltage, high speed power MOSFET and IGBT drivers with dependent high and low side referenced output channels. Proprietary HVIC and latch immune CMOS technologies enable ruggedized monolithic construction. The logic input is compatible with standard CMOS or LSTTL output, down to 3.3V logic. The output drivers feature a high pulse current buffer stage designed for minimum driver cross-conduction. The floating channel can be used to drive an N-channel power MOSFET or IGBT in the high side configuration which operates from 10 to 600 volts.

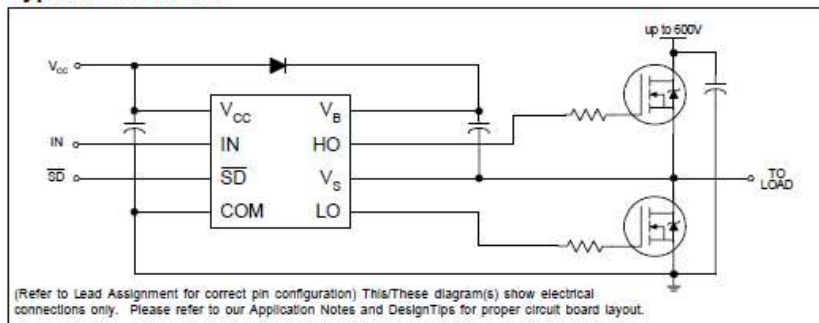
### Product Summary

V <sub>OFFSET</sub>	600V max.
I <sub>O+/-</sub>	130 mA / 270 mA
V <sub>OUT</sub>	10 - 20V
t <sub>on/off</sub> (typ.)	680 & 150 ns
Deadtime (typ.)	520 ns

### Packages



### Typical Connection



**Absolute Maximum Ratings**

Absolute maximum ratings indicate sustained limits beyond which damage to the device may occur. All voltage parameters are absolute voltages referenced to COM. The thermal resistance and power dissipation ratings are measured under board mounted and still air conditions.

Symbol	Definition	Min.	Max.	Units	
V <sub>B</sub>	High side floating absolute voltage	-0.3	625	V	
V <sub>S</sub>	High side floating supply offset voltage	V <sub>B</sub> - 25	V <sub>B</sub> + 0.3		
V <sub>HO</sub>	High side floating output voltage	V <sub>S</sub> - 0.3	V <sub>B</sub> + 0.3		
V <sub>CC</sub>	Low side and logic fixed supply voltage	-0.3	25		
V <sub>LO</sub>	Low side output voltage	-0.3	V <sub>CC</sub> + 0.3		
V <sub>IN</sub>	Logic input voltage (IN & $\overline{SD}$ )	-0.3	V <sub>CC</sub> + 0.3		
dV <sub>S</sub> /dt	Allowable offset supply voltage transient	—	50	V/ns	
P <sub>D</sub>	Package power dissipation @ T <sub>A</sub> ≤ +25°C	(8 lead PDIP)	—	1.0	W
		(8 lead SOIC)	—	0.625	
R <sub>thJA</sub>	Thermal resistance, junction to ambient	(8 lead PDIP)	—	125	°C/W
		(8 lead SOIC)	—	200	
T <sub>J</sub>	Junction temperature	—	150	°C	
T <sub>S</sub>	Storage temperature	-55	150		
T <sub>L</sub>	Lead temperature (soldering, 10 seconds)	—	300		

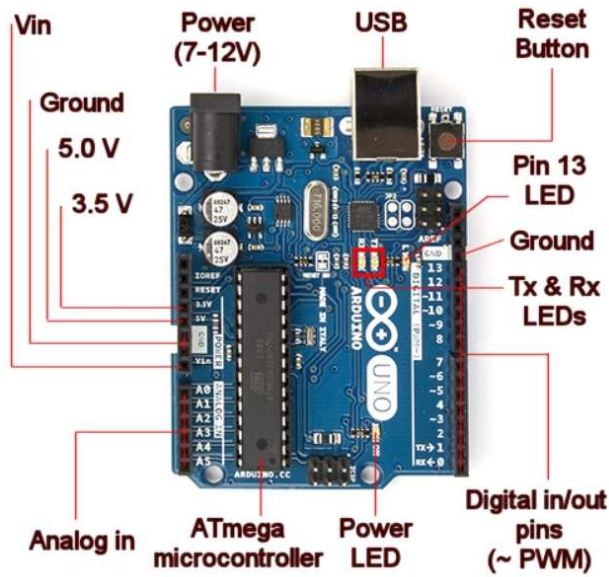
**Recommended Operating Conditions**

The Input/Output logic timing diagram is shown in Figure 1. For proper operation the device should be used within the recommended conditions. The V<sub>S</sub> offset rating is tested with all supplies biased at 15V differential.

Symbol	Definition	Min.	Max.	Units
V <sub>B</sub>	High side floating supply absolute voltage	V <sub>S</sub> + 10	V <sub>S</sub> + 20	V
V <sub>S</sub>	High side floating supply offset voltage	Note 1	600	
V <sub>HO</sub>	High side floating output voltage	V <sub>S</sub>	V <sub>B</sub>	
V <sub>CC</sub>	Low side and logic fixed supply voltage	10	20	
V <sub>LO</sub>	Low side output voltage	0	V <sub>CC</sub>	
V <sub>IN</sub>	Logic input voltage (IN & $\overline{SD}$ )	0	V <sub>CC</sub>	
T <sub>A</sub>	Ambient temperature	-40	125	°C

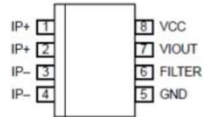
Note 1: Logic operational for V<sub>S</sub> of -5 to +600V. Logic state held for V<sub>S</sub> of -5V to -V<sub>BS</sub>. (Please refer to the Design Tip DT97-3 for more details).

## Appendix D Anatomy of Arduino UNO pin Functions

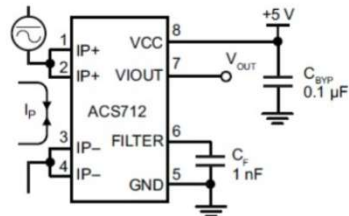


## Appendix E Current Sensor ACS217

Pin-out Diagram



Typical Application



Terminal List Table

Number	Name	Description
1 and 2	IP+	Terminals for current being sampled; fused internally
3 and 4	IP-	Terminals for current being sampled; fused internally
5	GND	Signal ground terminal
6	FILTER	Terminal for external capacitor that sets bandwidth
7	VIOUT	Analog output signal
8	VCC	Device power supply terminal

## Appendix F Test Load for Testing



## Appendix G Charge Controller MPPT Program

```
/*
#include <FastIO.h>
#include <I2CIO.h>
#include <LCD.h>
#include <LiquidCrystal.h>
#include <LiquidCrystal_I2C.h>
#include <LiquidCrystal_I2C_ByVac.h>
#include <LiquidCrystal_SI2C.h>
#include <LiquidCrystal_SR.h>
#include <LiquidCrystal_SR1W.h>
#include <LiquidCrystal_SR2W.h>
#include <LiquidCrystal_SR3W.h>
#include <SI2CIO.h>
#include <SoftI2CMaster.h>
*/
//-----
//
// ARDUINO SOLAR CHARGE CONTROLLER (MPPT)
//
//-----

#include "TimerOne.h" // using Timer1 library from http://www.arduino.cc/playground/Code/Timer1
#include <LiquidCrystal_I2C.h> // using the LCD I2C Library from https://bitbucket.org/fmalpartida/new-liquidcrystal/downloads
#include <Wire.h>
// SDA...>A4
// SCL...>A5
//-----
// definitions

#define SOL_AMPS_CHAN 0 // Defining the adc channel to read solar amps
#define SOL_VOLTS_CHAN 1 // defining the adc channel to read solar volts
```

```

#define BAT_VOLTS_CHAN 2          // defining the adc channel to read battery volts
#define AVG_NUM 100              // number of iterations of the adc routine to average the adc readings
#define SOL_AMPS_SCALE 0.0265    // the scaling value for raw adc reading to get solar amps // 5/(1024*0.185)
#define SOL_VOLTS_SCALE 0.0297  // the scaling value for raw adc reading to get solar volts // (5/1024)*(R1+R2)/R2
#define BAT_VOLTS_SCALE 0.0297  // the scaling value for raw adc reading to get battery volts
#define PWM_PIN 9                // the output pin for the pwm (only pin 9 available for timer 1 at 50kHz)
#define PWM_ENABLE_PIN 7        // pin used to control shutoff function of the IR2104 MOSFET driver (hight the mosfet
driver is on)
#define PWM_FULL 1023           // the actual value used by the Timer1 routines for 100% pwm duty cycle
#define PWM_MAX 100             // the value for pwm duty cycle 0-100%
#define PWM_MIN 60              // the value for pwm duty cycle 0-100% (below this value the current running in the system is
= 0)
#define PWM_START 90            // the value for pwm duty cycle 0-100%
#define PWM_INC 1               //the value the increment to the pwm value for the ppt algorithm
#define LOAD_BUTTON 0
#define TRUE 1
#define FALSE 0
#define ON TRUE
#define OFF FALSE
#define TURN_ON_MOSFETS digitalWrite(PWM_ENABLE_PIN, HIGH) // enable MOSFET driver
#define TURN_OFF_MOSFETS digitalWrite(PWM_ENABLE_PIN, LOW) // disable MOSFET driver
#define ONE_SECOND 50000       //count for number of interrupt in 1 second on interrupt period of 20us
#define LOW_SOL_WATTS 5.00      //value of solar watts // this is 5.00 watts
#define MIN_SOL_WATTS 1.00      //value of solar watts // this is 1.00 watts
#define MIN_BAT_VOLTS 8.80      //value of battery voltage // this is 9.80 volts
#define MAX_BAT_VOLTS 11.0      //value of battery voltage// this is 12.60 volts
#define HIGH_BAT_VOLTS 11.1     //value of battery voltage // this is 12.40 volts
#define LVD 10.5                //Low voltage disconnect setting for a 12V system
#define OFF_NUM 9               // number of iterations of off charger state
//-----
//Defining led pins for indication
#define LED_RED 10
#define LED_GREEN 11
#define LED_YELLOW 8
//-----
// Defining load control pin
#define LOAD_PIN 2 // pin-2 is used to control the load
//-----
// Defining lcd back light pin
#define BACK_LIGHT_PIN 5 // pin-2 is used to control the load
//-----
//////////////////////////////////BIT MAP ARRAY//////////////////////////////////
//-----
byte solar[8] = //icon for termometer
{
  0b11111,
  0b10101,
  0b11111,
  0b10101,
  0b11111,
  0b10101,
}

```

```

0b11111,
0b00000
};
byte battery[8]=
{
0b01110,
0b11011,
0b10001,
0b10001,
0b11111,
0b11111,
0b11111,
0b11111,
};
byte _PWM [8]=
{
0b11101,
0b10101,
0b10101,
0b10101,
0b10101,
0b10101,
0b10101,
0b10111,
};
//-----
// global variables
int buttonState = 0;    // variable for reading the pushbutton status
int count = 0;
int pwm = 0;           //pwm duty cycle 0-100%
float sol_amps;        // solar amps
float sol_volts;       // solar volts
float bat_volts;       // battery volts
float sol_watts;       // solar watts
float old_sol_watts = 0; // solar watts from previous time through ppt routine
unsigned int seconds = 0; // seconds from timer routine
unsigned int prev_seconds = 0; // seconds value from previous pass
unsigned int interrupt_counter = 0; // counter for 20us interrupt
boolean led_on = TRUE;
int led_counter = 0;
int delta = PWM_INC; // variable used to modify pwm duty cycle for the ppt algorithm
char ResetLCD;
enum charger_mode {off, on, bulk, bat_float} charger_state; // enumerated variable that holds state for charger state machine
// set the LCD address to 0x27 for a 20 chars 4 line display
// Set the pins on the I2C chip used for LCD connections:
//      addr, en,rw,rs,d4,d5,d6,d7,bl,b1pol
LiquidCrystal_I2C lcd(0x27, 2, 1, 0, 4, 5, 6, 7, 3, POSITIVE); // Set the LCD I2C address
//int back_light_Pin = 5;
//int load_pin =6;
int back_light_pin_State = 0;
int load_status=0;

```

```

//-----
// This routine is automatically called at powerup/reset
//-----
void setup()          // run once, when the sketch starts
{
  pinMode(LED_RED, OUTPUT);
  pinMode(LED_GREEN, OUTPUT);
  pinMode(LED_YELLOW, OUTPUT);
  pinMode(LOAD_BUTTON, INPUT);
  pinMode(PWM_ENABLE_PIN, OUTPUT); // sets the digital pin as output
  Timer1.initialize(20); // initialize timer1, and set a 20uS period
  Timer1.pwm(PWM_PIN, 0); // setup pwm on pin 9, 0% duty cycle
  TURN_OFF_MOSFETS; //turn off MOSFET driver chip
  Timer1.attachInterrupt(callback); // attaches callback() as a timer overflow interrupt
  Serial.begin(9600); // open the serial port at 38400 bps:
  pwm = PWM_START; //starting value for pwm
  charger_state = off; // start with charger state as off
  pinMode(BACK_LIGHT_PIN, INPUT);
  pinMode(LOAD_PIN,OUTPUT);
  digitalWrite(LOAD_PIN,LOW); // default load state is OFF
  digitalWrite(BACK_LIGHT_PIN,LOW); // default LCD back light is OFF
  lcd.begin(20,4); // initialize the lcd for 16 chars 2 lines, turn on backlight
  //lcd.noBacklight();
  lcd.createChar(1,solar);
  lcd.createChar(2,battery);
  lcd.createChar(3,_PWM);
  lcd.backlight();
  ResetLCD = 0;
}
//-----
// This is interrupt service routine for Timer1 that occurs every 20uS.
//
//-----
void callback()
{
  if (interrupt_counter++ > ONE_SECOND) { //increment interrupt_counter until one second has passed
    interrupt_counter = 0;
    seconds++; //then increment seconds counter
  }
}
//-----
// This routine reads and averages the analog inputs for this system, solar volts, solar amps and
// battery volts.
//-----
unsigned int read_adc(int channel){
  long sum = 0;
  int temp;
  int i;

  for (i=0; i<AVG_NUM; i++) { // loop through reading raw adc values AVG_NUM number of times
    temp = analogRead(channel); // read the input pin

```

```

    sum += temp;           // store sum for averaging
    delayMicroseconds(20); // pauses for 20 microseconds
}
return(sum / AVG_NUM);    // divide sum by AVG_NUM to get average and return it
}
//-----
// This routine uses the Timer1.pwm function to set the pwm duty cycle.
//-----
void set_pwm_duty(void) {
    if (pwm > PWM_MAX) { // check limits of PWM duty cycle and set to
PWM_MAX
        pwm = PWM_MAX;
    }
    else if (pwm < PWM_MIN) { // if pwm is less than PWM_MIN then set it to PWM_MIN
        pwm = PWM_MIN;
    }
    if (pwm < PWM_MAX) {
        Timer1.pwm(PWM_PIN,(PWM_FULL * (long)pwm / 100), 20); // use Timer1 routine to set pwm duty cycle at 20uS period
        //Timer1.pwm(PWM_PIN,(PWM_FULL * (long)pwm / 100));
    }

    else if (pwm == PWM_MAX) { // if pwm set to 100% it will be on full but we have
        Timer1.pwm(PWM_PIN,(PWM_FULL - 1), 1000); // keep switching so set duty cycle at 99.9% and slow down to
1000uS period
        //Timer1.pwm(PWM_PIN,(PWM_FULL - 1));
    }
}

//-----
// This routine prints all the data out to the serial port.
//-----
void print_data(void) {

    double temp;
    temp = interrupt_counter * 0.00002;
    temp *= 100;
    Serial.print(seconds,DEC);
    Serial.print(".");
    Serial.print(temp,0);
    Serial.print(" ");

    Serial.print("Charging = ");
    if (charger_state == on) Serial.print("on ");
    else if (charger_state == off) Serial.print("off ");
    else if (charger_state == bulk) Serial.print("bulk ");
    else if (charger_state == bat_float) Serial.print("float");
    Serial.print(" ");
    Serial.print("pwm = ");
    Serial.print(pwm,DEC);
    Serial.print(" ");
}

```



```

Serial.print("Current (panel) = ");
//print_int100_dec2(sol_amps);
Serial.print(sol_amps);
Serial.print("  ");
Serial.print("Voltage (panel) = ");
Serial.print(sol_volts);
//print_int100_dec2(sol_volts);
Serial.print("  ");
Serial.print("Power (panel) = ");
Serial.print(sol_watts);
// print_int100_dec2(sol_watts);
Serial.print("  ");
Serial.print("Battery Voltage = ");
Serial.print(bat_volts);
//print_int100_dec2(bat_volts);
Serial.print("  ");
Serial.print("\n\n");
delay(1000);
}
//-----
// This routine reads all the analog input values for the system. Then it multiplies them by the scale
// factor to get actual value in volts or amps.
//-----
void read_data(void) {
  sol_amps = (read_adc(SOL_AMPS_CHAN) * SOL_AMPS_SCALE) - 13.34; //input of solar amps
  if(sol_amps < 0) {sol_amps = 0;}
  sol_volts = read_adc(SOL_VOLTS_CHAN) * SOL_VOLTS_SCALE; //input of solar volts
  bat_volts = read_adc(BAT_VOLTS_CHAN) * BAT_VOLTS_SCALE; //input of battery volts
  sol_watts = sol_amps * sol_volts ; //calculations of solar watts
}
//-----
// This routine is the charger state machine. It has four states on, off, bulk and float.
// It's called once each time through the main loop to see what state the charger should be in.
// The battery charger can be in one of the following four states:
//
// On State - this is charger state for MIN_SOL_WATTS < solar watts < LOW_SOL_WATTS. In this state is the solar
// watts input is too low for the bulk charging state but not low enough to go into the off state.
// In this state we just set the pwm = 99.9% to get the most of low amount of power available.
// Bulk State - this is charger state for solar watts > MIN_SOL_WATTS. This is where we do the bulk of the battery
// charging and where we run the Peak Power Tracking algorithm. In this state we try and run the maximum amount
// of current that the solar panels are generating into the battery.
// Float State - As the battery charges it's voltage rises. When it gets to the MAX_BAT_VOLTS we are done with the
// bulk battery charging and enter the battery float state. In this state we try and keep the battery voltage
// at MAX_BAT_VOLTS by adjusting the pwm value. If we get to pwm = 100% it means we can't keep the battery
// voltage at MAX_BAT_VOLTS which probably means the battery is being drawn down by some load so we need to back
// into the bulk charging mode.
// Off State - This is state that the charger enters when solar watts < MIN_SOL_WATTS. The charger goes into this
// state when there is no more power being generated by the solar panels. The MOSFETs are turned
// off in this state so that power from the battery doesn't leak back into the solar panel.
//-----

```

```

void run_charger(void) {
    static int off_count = OFF_NUM;

    switch (charger_state) {
    case on:
        if (sol_watts < MIN_SOL_WATTS) {           //if watts input from the solar panel is less than
            charger_state = off;                   //the minimum solar watts then
            off_count = OFF_NUM;                   //go to the charger off state
            TURN_OFF_MOSFETS;
        }
        else if (bat_volts > MAX_BAT_VOLTS) {      //else if the battery voltage has gotten above the float
            charger_state = bat_float;             //battery float voltage go to the charger battery float state
        }
        else if (sol_watts < LOW_SOL_WATTS) {      //else if the solar input watts is less than low solar watts
            pwm = PWM_MAX;                         //it means there is not much power being generated by the solar panel
            set_pwm_duty();                         //so we just set the pwm = 100% so we can get as much of this power as
possible
            ResetLCD = 1;
        }
        //and stay in the charger on state
        else {
            pwm = ((bat_volts * 10) / (sol_volts / 10)) + 5; //else if we are making more power than low solar watts figure out what
the pwm
            charger_state = bulk;                   //value should be and change the charger to bulk state
        }
        break;
    case bulk:
        if (sol_watts < MIN_SOL_WATTS) {           //if watts input from the solar panel is less than
            charger_state = off;                   //the minimum solar watts then it is getting dark so
            off_count = OFF_NUM;                   //go to the charger off state
            TURN_OFF_MOSFETS;
        }
        else if (bat_volts > MAX_BAT_VOLTS) {      //else if the battery voltage has gotten above the float
            charger_state = bat_float;             //battery float voltage go to the charger battery float state
        }
        else if (sol_watts < LOW_SOL_WATTS) {      //else if the solar input watts is less than low solar watts
            charger_state = on;                   //it means there is not much power being generated by the solar panel
            TURN_ON_MOSFETS;                       //so go to charger on state
        }
        else {
            // this is where we do the Peak Power Tracking ro Maximum Power Point algorithm
            if (old_sol_watts >= sol_watts) {      // if previous watts are greater change the value of
                delta = -delta;                    // delta to make pwm increase or decrease to maximize watts
            }
            pwm += delta;                          // add delta to change PWM duty cycle for PPT algorithm (compound addition)
            old_sol_watts = sol_watts;             // load old_watts with current watts value for next time
            set_pwm_duty();                         // set pwm duty cycle to pwm value
            ResetLCD = 1;
        }
        break;
    case bat_float:
        if (sol_watts < MIN_SOL_WATTS) {           //if watts input from the solar panel is less than
            charger_state = off;                   //the minimum solar watts then it is getting dark so

```

```

    off_count = OFF_NUM;          //go to the charger off state
    set_pwm_duty();
    TURN_OFF_MOSFETS;
}
else if (bat_volts > MAX_BAT_VOLTS) { //since we're in the battery float state if the battery voltage
    pwm -= 1;                      //is above the float voltage back off the pwm to lower it
    set_pwm_duty();
}
else if (bat_volts < MAX_BAT_VOLTS) { //else if the battery voltage is less than the float voltage
    pwm += 1;                      //increment the pwm to get it back up to the float voltage
    set_pwm_duty();
    if (pwm >= 100) {              //if pwm gets up to 100 it means we can't keep the battery at
        charger_state = bulk;      //float voltage so jump to charger bulk state to charge the battery
    }
}
break;
case off:                          //when we jump into the charger off state, off_count is set with OFF_NUM
    if (off_count > 0) {           //this means that we run through the off state OFF_NUM of times with out doing
        off_count--;              //anything, this is to allow the battery voltage to settle down to see if the
    }                              //battery has been disconnected
    else if ((bat_volts > HIGH_BAT_VOLTS) && (bat_volts < MAX_BAT_VOLTS) && (sol_volts > bat_volts)) {
        charger_state = bat_float; //if battery voltage is still high and solar volts are high
        set_pwm_duty();            //change charger state to battery float
        TURN_ON_MOSFETS;
    }
    else if ((bat_volts > MIN_BAT_VOLTS) && (bat_volts < MAX_BAT_VOLTS) && (sol_volts > bat_volts)) {
        pwm = PWM_START;          //if battery volts aren't quite so high but we have solar volts
        set_pwm_duty();           //greater than battery volts showing it is day light then
        charger_state = on;       //change charger state to on so we start charging
        TURN_ON_MOSFETS;
    }                              //else stay in the off state
    break;
default:
    TURN_OFF_MOSFETS;
    break;
}
}
//-----
// Main loop.
//
//-----
void loop()
{
    read_data();                  //read data from inputs
    run_charger();                //run the charger state machine
    print_data();                 //print data
    load_control();              // control the connected load
    led_output();                 // led indication
    lcd_display();               // lcd display
    if(ResetLCD == 1)
    {

```

```

    lcd.begin(20,4); // initialize the lcd for 16 chars 2 lines, turn on backlight
    //lcd.noBacklight();
    lcd.backlight();
    lcd.createChar(1,solar);
    lcd.createChar(2,battery);
    lcd.createChar(3,_PWM);
    ResetLCD = 0;
    lcd_display();          // lcd display
}
}

//-----
//
//This function displays the curnnet state with the help of the 3 LEDs
//
//-----
//-----
////////////////////////////////////LOAD CONTROL////////////////////////////////////
//-----

void load_control()
{
    buttonState = digitalRead(LOAD_BUTTON);
    if (buttonState == LOW) // if load switch is turned on
    {
        if(bat_volts >LVD) // check if battery is healthy
        {
            load_status=1;
            digitalWrite(LOAD_PIN, HIGH); // load is ON
        }
        else if(bat_volts < LVD)
        {
            load_status=0;
            digitalWrite(LOAD_PIN, LOW); //load is OFF
        }
    }
    else // load will off during day
    {
        load_status=0;
        digitalWrite(LOAD_PIN, LOW);
    }
}

//-----
//-----Led Indication-----
//-----

void led_output(void)
{
    if(bat_volts >= MAX_BAT_VOLTS)
    {
        leds_off_all();
    }
}

```

```

    digitalWrite(LED_YELLOW, HIGH);
}
else if(bat_volts > MIN_BAT_VOLTS && bat_volts < MAX_BAT_VOLTS)
{
    leds_off_all();
    digitalWrite(LED_GREEN, HIGH);
}
else if(bat_volts <= MIN_BAT_VOLTS)
{
    leds_off_all();
    digitalWrite(LED_RED, HIGH);
}
}

//-----
//
// This function is used to turn all the leds off
//
//-----
void leds_off_all(void)
{
    digitalWrite(LED_GREEN, LOW);
    digitalWrite(LED_RED, LOW);
    digitalWrite(LED_YELLOW, LOW);
}
//----- LCD DISPLAY -----
//-----
void lcd_display()
{
    float diff_Batt, Batt_Lvl1, Batt_Lvl2, Batt_Lvl3, Batt_Lvl4, Batt_Lvl5, Batt_Lvl6, Batt_Lvl7, Batt_Lvl8;
    diff_Batt = MAX_BAT_VOLTS - MIN_BAT_VOLTS;
    diff_Batt = diff_Batt / 8;
    Batt_Lvl1 = MAX_BAT_VOLTS - diff_Batt;
    Batt_Lvl2 = Batt_Lvl1 - diff_Batt;
    Batt_Lvl3 = Batt_Lvl2 - diff_Batt;
    Batt_Lvl4 = Batt_Lvl3 - diff_Batt;
    Batt_Lvl5 = Batt_Lvl4 - diff_Batt;
    Batt_Lvl6 = Batt_Lvl5 - diff_Batt;
    Batt_Lvl7 = Batt_Lvl6 - diff_Batt;
    Batt_Lvl8 = Batt_Lvl7 - diff_Batt;

    back_light_pin_State = digitalRead(BACK_LIGHT_PIN);
    if (back_light_pin_State == HIGH)
    {
        lcd.backlight();// finish with backlight on
        // Wait for 10 seconds and then turn off the display and backlight.
        delay(15000);
        lcd.noBacklight();
    }
}

```

```

lcd.setCursor(0, 0);
lcd.print("SOL");
lcd.setCursor(4, 0);
lcd.write(1);
lcd.setCursor(0, 1);
lcd.print(sol_volts);
lcd.print("V ");
lcd.setCursor(0, 2);
lcd.print(sol_amps);
lcd.print("A ");
lcd.setCursor(0, 3);
lcd.print(sol_watts);
lcd.print("W ");
lcd.setCursor(8, 0);
lcd.print("BAT");
lcd.setCursor(12, 0);
lcd.write(2);
lcd.setCursor(8, 1);
lcd.print(bat_volts);
lcd.setCursor(8,2);

if (charger_state == on)
lcd.print("On ");
else if (charger_state == off)
lcd.print("off ");
else if (charger_state == bulk)
lcd.print("bulk ");
else if (charger_state == bat_float)
lcd.print("float");

//-----
//-----Battery State Of Charge -----
//-----

lcd.setCursor(8,3);

if ( bat_volts >= MAX_BAT_VOLTS)
{
  lcd.print( "100%");
}
else if (bat_volts >= Batt_Lvl1 && bat_volts < MAX_BAT_VOLTS)
{
  lcd.print( " 90%");
}
else if (bat_volts >= Batt_Lvl2 && bat_volts < Batt_Lvl1)
{
  lcd.print( " 80%");
}
else if (bat_volts >= Batt_Lvl3 && bat_volts < Batt_Lvl2)
{

```

```

lcd.print( " 70%");
}
else if (bat_volts >= Batt_Lvl4 && bat_volts < Batt_Lvl3)
{
  lcd.print( " 60%");
}
else if (bat_volts >= Batt_Lvl5 && bat_volts < Batt_Lvl4)
{
  lcd.print( " 50%");
}
else if (bat_volts >= Batt_Lvl6 && bat_volts < Batt_Lvl5)
{
  lcd.print( " 40%");
}
else if (bat_volts >= Batt_Lvl7 && bat_volts < Batt_Lvl6)
{
  lcd.print( " 30%");
}
else if (bat_volts >= Batt_Lvl8 && bat_volts < Batt_Lvl7)
  lcd.print( " 20%");
else if (bat_volts >= MIN_BAT_VOLTS && bat_volts < Batt_Lvl8)
  lcd.print( " 10%");
else if (bat_volts < MIN_BAT_VOLTS)
  lcd.print( " 0%");

//-----
//-----Duty Cycle-----
//-----
lcd.setCursor(15,0);
lcd.print("PWM");
lcd.setCursor(19,0);
lcd.write(3);
lcd.setCursor(15,1);
lcd.print(pwm);
lcd.print("%");
//-----
//-----Load Status-----
//-----
lcd.setCursor(15,2);
lcd.print("Load");
lcd.setCursor(15,3);
if (load_status == 1)
{
  lcd.print("On ");
}
else
{
  lcd.print("Off");
}
}

```

## Appendix H LCD and Data Logger

### H.1 LCD Code

```
// Get the LCD I2C Library here:
// https://bitbucket.org/fmalpartida/new-liquidcrystal/downloads
// SDA...>A4
// SCL...>A5
#include <LiquidCrystal_I2C.h>
#include <Wire.h>
byte solar[8] = //icon for termometer
{
    0b11111,
    0b10101,
    0b11111,
    0b10101,
    0b11111,
    0b10101,
    0b11111,
    0b00000
};

byte battery[8]=
{
    0b01110,
    0b11011,
    0b10001,
    0b10001,
    0b11111,
    0b11111,
    0b11111,
    0b11111,
};

byte pwm [8]=
{
    0b11101,
    0b10101,
    0b10101,
    0b10101,
    0b10101,
    0b10101,
    0b10101,
    0b10111,
};

int temp=0;
float sum =0;
float AMPS_SCALE =0;
float amps=0;
```



```

// set the LCD address to 0x27 for a 20 chars 4 line display
// Set the pins on the I2C chip used for LCD connections:
//          addr, en,rw,rs,d4,d5,d6,d7,bl,blpol
LiquidCrystal_I2C lcd(0x27, 2, 1, 0, 4, 5, 6, 7, 3, POSITIVE); // Set the LCD I2C address
int backlight_Pin = 5;
int backlight_State = 0;
void setup() /*----( SETUP: RUNS ONCE )----*/
{
  Serial.begin(9600); // Used to type in characters
  pinMode(backlight_Pin, INPUT);
  lcd.begin(20,4); // initialize the lcd for 16 chars 2 lines, turn on backlight
  lcd.noBacklight();
  lcd.createChar(1,solar);
  lcd.createChar(2, battery);
  lcd.createChar(3, pwm);

  //----- Write characters on the display -----
  // NOTE: Cursor Position: (CHAR, LINE) start at 0

  lcd.clear();

}/*--(end setup )--*/

void loop()
{
  symbol();
  backlight_State = digitalRead(backlight_Pin);
  if ( backlight_State == HIGH)
  {
    lcd.backlight();// finish with backlight on
  }
  // Wait for 10 seconds and then turn off the display and backlight.
  lcd.noBacklight();
}

for(int i = 0; i < 100; i++) // loop through reading raw adc values 100 number of times
{
  temp=analogRead(A1); // read the input pin
  sum += temp; // store sum for averaging
  delayMicroseconds(50);
}
sum=sum/100; // divide sum by 100 to get average

// Calibration for current

AMPS_SCALE= 0.00488/ 0.185; //5/1024 = 0.00488 // Sensitivity = 185mV
amps = AMPS_SCALE* sum - 13.51; // 2.5/0.185 = 13.51

lcd.setCursor(0, 2);

```

```

    lcd.print(amps);
    delay(500);
}
void symbol()

{
  lcd.setCursor(0, 0);
  lcd.print("SOL");
  lcd.setCursor(4, 0);
  lcd.write(1);
  lcd.setCursor(0, 1);
  lcd.print("16.45V");
  lcd.setCursor(0, 2);
  lcd.print("1.03A");
  lcd.setCursor(0, 3);
  lcd.print("16.94W");
  lcd.setCursor(8, 0);
  lcd.print("BAT");
  lcd.setCursor(12, 0);
  lcd.write(2);
  lcd.setCursor(8, 1);
  lcd.print("12.35V");
  lcd.setCursor(8,2);
  lcd.print("bulk");
  lcd.setCursor(8,3);
  lcd.print("70%");

  lcd.setCursor(15,0);
  lcd.print("PWM");
  lcd.setCursor(19,0);
  lcd.write(3);
  lcd.setCursor(15,1);
  lcd.print("95%");

  lcd.setCursor(15,2);
  lcd.print("Load");
  lcd.setCursor(15,3);
  lcd.print("Off");
}

```

## H.2 Data Logger Code

```

#include "TimerOne.h"          // using Timer1 library from http://www.arduino.cc/playground/Code/Timer1
#include <LiquidCrystal_I2C.h> // using the LCD I2C Library from https://bitbucket.org/fmalpartida/new-liquidcrystal/downloads
#include <Wire.h>
#define CURRCH1 0             // Defining the adc channel to read ch0
#define VOLTCH1 1            // defining the adc channel to read ch1
#define CURRCH2 2            // Defining the adc channel to read ch2
#define VOLTCH2 3            // defining the adc channel to read ch3
#define CURRCH3 4            // Defining the adc channel to read ch4

```

```

#define VOLTCH3 5          // defining the adc channel to read ch5
#define AVG_NUM 8         // number of iterations of the adc routine to average the adc readings
#define AMPS_SCALE 0.0257 // the scaling value for raw adc reading to get amps // 5/(1024*0.185)
#define VOLTS_SCALE 0.0289 // the scaling value for raw adc reading to get volts // (5/1024)*(R1+R2)/R2
#define TRUE 1
#define FALSE 0
#define ON TRUE
#define OFF FALSE
#define ONE_SECOND 50000
// global variables 20 SEPT 2016
int count = 0;
float Curr1;           //current measurement 1
float Curr2;           //current measurement 2
float Curr3;           //current measurement 3
float Volt1;           //voltage measurement 1
float Volt2;           //voltage measurement 2
float Volt3;           //voltage measurement 3
unsigned int seconds = 0; // seconds from timer routine
unsigned int prev_seconds = 0; // seconds value from previous pass
unsigned int interrupt_counter = 0; // counter for 20us interrupt
unsigned long time = 1;
//-----
// This is interrupt service routine for Timer1 that occurs every 20uS.
//
//-----
void callback()
{
  if(interrupt_counter++ > ONE_SECOND) { //increment interrupt_counter until one second has passed
    interrupt_counter = 0;
    seconds++; //then increment seconds counter
  }
}
//-----
// This routine is automatically called at powerup/reset
//-----
void setup() // run once, when the sketch starts
{
  Timer1.initialize(20); // initialize timer1, and set a 20uS period
  Timer1.attachInterrupt(callback); // attaches callback() as a timer overflow interrupt
  Serial.begin(9600); // open the serial port at 9600 bps:
}
//-----
// This routine reads and averages the analog inputs
//-----
int read_adc(int channel) {
  int sum = 0;
  int temp;
  int i;
  for (i = 0; i < AVG_NUM; i++) { // loop through reading raw adc values AVG_NUM number of times
    temp = analogRead(channel); // read the input pin
    sum += temp; // store sum for averaging
  }
}

```

```

    delayMicroseconds(50);      // pauses for 50 microseconds
}
return (sum / AVG_NUM);        // divide sum by AVG_NUM to get average and return it
}
//-----
// This routine prints all the data out to the serial port.
//-----
void print_data(void)
{
    double temp;
    temp = interrupt_counter * 0.00002;
    temp *=100;
    Serial.print("Time = ");
    Serial.print(seconds,DEC);
    Serial.print(".");
    Serial.print(temp, 0);
    Serial.print(" , ");
    Serial.print("Current Panel = ");
    Serial.print(Curr1);
    Serial.print(" , ");
    Serial.print("Voltage Panel = ");
    Serial.print(Volt1);
    Serial.print(" , ");
    Serial.print("Current Battery = ");
    Serial.print(Curr2);
    Serial.print(" , ");

    Serial.print("Voltage Battery = ");
    Serial.print(Volt2);
    Serial.print(" , ");
    Serial.print("Current Load = ");
    Serial.print(Curr3);
    Serial.print(" , ");
    Serial.print("Voltage Lload = ");
    Serial.print(Volt3);
    Serial.print(" , ");
    Serial.print (temp,0);
    Serial.print(" , ");
    Serial.print("\r");
    //delay(1000);
}
//-----
// This routine reads all the analog input values for the system. Then it multiplies them by the scale
// factor to get actual value in volts or amps.
//-----
void read_data(void) {

    Curr1 = (read_adc(CURRCH1) * AMPS_SCALE - 13.52); //input of solar amps
    Curr1 = Curr1 * 2; //input of solar amps
    Volt1 = read_adc(VOLTCH1) * VOLTS_SCALE; //input of solar volts
    Curr2 = (read_adc(CURRCH2) * AMPS_SCALE - 13.52); //input of solar amps

```

```

Curr2 = Curr2 * 2; //input of solar amps
Volt2 = read_adc(VOLTCH2) * VOLTS_SCALE; //input of solar volts
Curr3 = (read_adc(CURRCH3) * AMPS_SCALE - 13.52); //input of solar amps
Curr3 = Curr3 * 2; //input of solar amps
Volt3 = read_adc(VOLTCH3) * VOLTS_SCALE; //input of solar volts
}
//-----
// Main loop.
//
//-----
void loop()
{
  read_data(); //read data from inputs
  print_data(); //print data
}

```

## Appendix I Results Data

### I.1 Experiments E1 at Irradiance 380 W/m<sup>2</sup>

Time (sec)	Panel Power (W)	Irradiance (W/sqm)	Duty Cycle D	Step Size	Output Voltage (V)
1905.69	30.7530	380	0.600884	0.0009948	10.87
1905.81	27.9000	380	0.605556	0.0046711	10.90
1905.93	29.8980	380	0.599890	-0.0056659	10.87
1906.40	31.7100	380	0.599890	0.0000000	10.87
1906.16	31.6050	380	0.603544	0.0036541	10.90
1906.28	28.1790	380	0.597910	-0.0056340	10.87
1906.39	29.1360	380	0.595277	-0.0026325	10.84
1906.51	28.1325	380	0.598898	0.0036208	10.87
1906.63	26.0928	380	0.599890	0.0009916	10.87
1906.75	29.1360	380	0.596925	-0.0029649	10.87
1906.86	28.9920	380	0.598234	0.0013092	10.84
1906.98	29.0400	380	0.598898	0.0006641	10.87
1907.10	26.9988	380	0.599890	0.0009916	10.87
1907.22	31.8150	380	0.597910	-0.0019798	10.87
1907.33	28.0860	380	0.599890	0.0019798	10.87
1907.45	28.1790	380	0.597910	-0.0019798	10.87
1907.57	28.0860	380	0.599890	0.0019798	10.87
1907.69	29.8485	380	0.600884	0.0009948	10.87
1907.80	30.7020	380	0.603544	0.0026593	10.90
1907.92	28.9920	380	0.599890	-0.0036541	10.87
1908.40	29.0400	380	0.598898	-0.0009916	10.87
1908.15	28.9440	380	0.600884	0.0019864	10.87
1908.27	26.8647	380	0.604548	0.0036635	10.90
1908.39	28.0860	380	0.599890	-0.0046584	10.87
1908.51	28.9440	380	0.600884	0.0009948	10.87

### I.1 Experiments E1 at Irradiance 665 W/m<sup>2</sup>

Time (sec)	Panel Power (W)	Irradiance (W/sqm)	Duty Cycle D	Step Size	Output Voltage (V)
3875.13	35.7204	665	0.629758	-0.0021867	10.92
3875.25	35.1848	665	0.644614	0.0148558	11.01
3875.37	33.7120	665	0.638372	-0.0062415	10.98
3875.49	33.6532	665	0.641235	0.0028626	11.01
3875.60	36.2287	665	0.641235	0.0000000	11.01
3875.72	32.8520	665	0.640116	-0.0011184	11.01
3875.84	34.6122	665	0.639373	-0.0007435	11.01
3875.96	35.3084	665	0.642357	0.0029842	11.01
3876.70	34.5117	665	0.641235	-0.0011223	11.01
3876.19	35.4320	665	0.640116	-0.0011184	11.01
3876.31	35.3084	665	0.642357	0.0022408	11.01
3876.42	34.3308	665	0.646370	0.0040130	11.04
3876.54	32.0235	665	0.630849	-0.0155208	10.92
3876.66	33.8688	665	0.633681	0.0028313	10.95
3876.78	33.0048	665	0.633681	0.0000000	10.95
3876.89	29.4270	665	0.630849	-0.0028313	10.92
3877.10	33.9864	665	0.629758	-0.0010914	10.92
3877.13	34.7328	665	0.633681	0.0039228	10.95
3877.25	32.9475	665	0.634783	0.0011021	10.95
3877.36	34.8534	665	0.629758	-0.0050248	10.92
3877.48	38.1888	665	0.631944	0.0021867	10.92
3877.60	31.8570	665	0.634146	0.0022019	10.92
3877.72	32.3380	665	0.621854	-0.0122928	10.87
3877.83	33.3486	665	0.620848	-0.0010059	10.84
3877.95	34.1628	665	0.623637	0.0027898	10.87

## I2 Experiment E2 at Irradiance 710 W/m<sup>2</sup>

Irradiance (W/sqm)	Duty Cycle D	Step Size	Output Voltage (V)	Current Load (A)	Output Power (W)
710	0.728000	0.0000000	10.92	1.03	11.2476
710	0.728000	0.0000000	10.92	1.08	11.7936
710	0.730924	0.0029237	10.92	0.98	10.7016
710	0.729459	-0.0014648	10.92	1.03	11.2476
710	0.728000	-0.0014589	10.92	1.08	11.7936
710	0.729585	0.0015850	10.90	0.93	10.1370
710	0.728000	-0.0015850	10.92	1.03	11.2476
710	0.726667	-0.0013333	10.90	1.08	11.7720
710	0.721268	-0.0053985	10.92	1.08	11.7936
710	0.718421	-0.0028471	10.92	0.98	10.7016
710	0.718523	0.0001023	10.90	1.08	11.7720
710	0.719947	0.0014238	10.90	1.08	11.7720
710	0.718523	-0.0014238	10.90	1.13	12.3170
710	0.722700	0.0041768	10.92	0.98	10.7016
710	0.723772	0.0010714	10.90	1.08	11.7720
710	0.719947	-0.0038244	10.90	0.98	10.6820
710	0.719947	0.0000000	10.90	1.13	12.3170
710	0.721377	0.0014294	10.90	0.98	10.6820
710	0.719947	-0.0014294	10.90	1.13	12.3170
710	0.715693	-0.0042544	10.90	1.13	12.3170
710	0.717105	0.0014126	10.90	1.13	12.3170
710	0.714286	-0.0028195	10.90	1.03	11.2270
710	0.717105	0.0028195	10.90	1.13	12.3170
710	0.715693	-0.0014126	10.90	1.08	11.7720
710	0.714286	-0.0014070	10.90	1.13	12.3170
710	0.715693	0.0014070	10.90	1.13	12.3170
710	0.717105	0.0014126	10.90	0.98	10.6820
710	0.714286	-0.0028195	10.90	1.08	11.7720
710	0.717105	0.0028195	10.90	1.13	12.3170
710	0.715693	-0.0014126	10.90	1.13	12.3170
710	0.715693	0.0000000	10.90	1.08	11.7720



### I.3 Experiment E3 at Irradiance 800 W/m<sup>2</sup>

Time (sec)	Power Panel (W)	Irradince (W/sqm)	Load Voltage (V)	Dury Cycle D	Step Size
1009.67	10.5648	800	11.27	0.992077465	0
1009.79	9.9968	800	11.27	0.992077465	0
1009.91	8.7472	800	11.27	0.992077465	0
1010.2	8.7472	800	11.27	0.992077465	0
1010.14	11.1034	800	11.24	0.992056487	-2.09776E-05
1010.38	45.115	800	11.88	0.921644686	-0.001971838
1010.49	42.2107	800	11.88	0.925954793	0.004310108
1010.61	42.9524	800	11.88	0.923794712	-0.002160081
1010.73	44.367	800	11.85	0.921461897	-0.002332815
1010.85	44.905	800	11.88	0.925954793	0.004492896
1010.96	44.367	800	11.85	0.921461897	-0.004492896
1011.8	43.622	800	11.85	0.923616524	0.002154626
1011.2	44.367	800	11.85	0.921461897	-0.002154626
1011.31	44.905	800	11.85	0.923616524	0.002154626

### I.3 Experiment E3 at Irradiance 850 W/m<sup>2</sup>

Time (sec)	Power Panel (W)	Irradince (W/sqm)	Load Voltage (V)	Dury Cycle D	Step Size
999.2	10.7508	850	11.88	0.987889273	-0.007740097
999.14	8.2584	850	11.88	0.993025283	0.00513601
999.26	10.6671	850	11.88	0.993025283	0
999.37	10.0936	850	11.85	0.993025283	0
999.49	10.0936	850	11.88	0.993025283	0
999.61	10.6671	850	11.88	0.990409765	-0.002615519
999.73	10.6392	850	11.88	0.993006993	0.002597228
999.84	10.0936	850	11.88	0.993025283	1.82903E-05
1000.8	49.2252	850	11.88	0.917182663	-0.002321981
1000.2	49.3395	850	11.88	0.917374517	0.000191855
1000.31	46.512	850	11.91	0.919504644	0.002130127
1000.43	46.728	850	11.88	0.915254237	-0.004250407
1000.55	49.7554	850	11.88	0.9193173	0.004063063
1000.67	47.915	850	11.88	0.917374517	-0.001942783
1000.79	47.804	850	11.88	0.919504644	0.002130127
1000.91	47.915	850	11.88	0.917374517	-0.002130127
1001.3	46.512	850	11.88	0.917182663	-0.000191855

## LIST OF PUBLICATIONS

### Journal with Impact Factor

1. **Dolah, A.**, Wahab, Y., Ghani, R. A., Yusof, A., Ngah, N. A., & Muhammad, N. F. I. (2015) Electrical Characteristics of Photovoltaic Cell Module by Simulation, *Applied Mechanics and Materials* ISSN: 1662-7482, Vol. 793, pp 358-362 doi:10.4028/www.scientific.net/AMM.793.358© 2015 Trans Tech Publications, Switzerland

### Conference Proceedings

1. **Dolah, A.**, Wahab, Y., Rahman, H. A., Yusof, A., Ngah, N. A., & Muhammad, N. F. I. (2013) Model Verification of the Electrical Performance of Photovoltaic Cell Module by Simulation, *Alternative Energy in Developing Countries and Emerging Economics*. Series: Energy Procedia Volume 52 ISBN: 9781634392501, Pages: 675 (1 Vol).
2. **Dolah, A.**, Wahab, Y., Ghani, R. A., Yusof, A., Ngah, N. A., & Muhammad, N. F. I. (2014) Electrical Characteristics of Photovoltaic Cell Module by Simulation, *International Conference Electrical Power Engineering and Application* ISBN: 3-0357-0073-7, ISBN: 3-03835-598-4, Scientific.Net, Materials Science & Engineering, Pfaffikon, Switzerland: Trans Tech Publications.